nature chemistry

SUPPLEMENTARY INFORMATION

https://doi.org/10.1038/s41557-019-0325-7

In the format provided by the authors and unedited.

Super-resolution labelling with Action-PAINT

Ninning Liu[1,3], Mingjie Dai[1,2,3]*, Sinem K. Saka[1] and Peng Yin[1,2]*

[1]Wyss Institute for Biologically Inspired Engineering, Harvard University, Boston, MA, USA. [2]Department of Systems Biology, Harvard Medical School, Boston, MA, USA. [3]These authors contributed equally: Ninning Liu, Mingjie Dai. *e-mail: mingjie_dai@hms.harvard.edu; py@hms.harvard.edu

Supplementary Materials

Super-resolution labelling with Action-PAINT

Ninning Liu[1,3], Mingjie Dai[1,2,3,*], Sinem K. Saka[1], Peng Yin[1,2,*]

[1]Wyss Institute for Biologically Inspired Engineering, Harvard University, Boston, MA 02115

[2]Department of Systems Biology, Harvard Medical School, Boston, MA 02115

[3]These authors contributed equally to this work

*Correspondence to: py@hms.harvard.edu (P.Y.); mingjie_dai@hms.harvard.edu (M.D.)

Table of contents

1. Materials 2
2. Methods 2
3. Notes 8
4. Figures 15
5. Tables 33

1. Materials

The following materials and buffers were used for oligo labelling, imaging and synthesis of synthetic DNA nanostructures. Unmodified, thiol-modified and biotin-labelled DNA oligonucleotides were purchased from Integrated DNA Technologies. Fluorescently modified DNA oligonucleotides were purchased from Biosynthesis. M13mp18 scaffold (N4040S) was purchased from New England BioLabs. DNA origami folding buffer used: 12.5 mM $MgCl_2$, 1x TE buffer.

The following materials and buffers were used for synthesis and purification of CNVK-bearing and fluorophore-labelled oligonucleotide strands. Deoxynucleoside phosphoramidites (10-1000, 10-1015, 10-1029, 10-1030), 3' - PT-Amino-Mod C3 CPG column (20-2954-41E), Glen-Pak column, and triethylamine acetate (TEAA, 60-4110) were purchased from Glen Research. 3-cyanovinylcarbazole (CNVK) phosphoramidite was purchased from Carbosynth (PC31915). Dimethyl sulfoxide (DMSO, 276855), acetonitrile (271004) and atto655 NHS ester (76245) were purchased from Sigma-Aldrich. Illustra NAP-5 column (17-0853-02) and cy3b NHS ester (PA63101) were purchased from GE Healthcare. Xterra MS C18 2.5 um column (186000602) was purchased from Waters.

The following materials and buffers were used for sample preparation of super-resolution fluorescence microscopy. Streptavidin was purchased from Invitrogen (S-888). Biotinylated bovine serum albumin (BSA-biotin, A8549), Protocatechuate 3,4-Dioxygenase (PCD, P8279), Protocatechuic acid (PCA, 37580) and 6-Hydroxy-2,5,7,8-tetramethylchromane-2-carboxylic acid (Trolox, 238813) were purchased from Sigma-Aldrich. Glass slides and coverslips were purchased from VWR. Imaging buffers used: buffer A (10 mM Tris-HCl, 100 mM NaCl, 0.1% (v/v) Tween 20, pH 8.0), buffer B (10 mM Tris-HCl, 10 mM $MgCl_2$, 1 mM EDTA, 0.1% Tween 20, pH 8.0) and buffer TP (1x buffer B, 10 nM PCD, 2.5 mM PCA, 1mM Trolox).

The following materials and buffers were used for microtubule immunostaining and super-resolution labelling. Rat anti-alpha-tubulin antibody YL1/2 (MA1-80017), SM(PEG)2 (PEGylated SMCC crosslinker, 22102), BS(PEG)5 (PEGylated bis(sulfosuccinimidyl)suberate, 21581), sheared salmon sperm DNA (AM9680) and Zeba spin desalting columns (7k MWCO, 89882) were purchased from Thermo Fisher. Donkey anti-rat IgG (H+L) antibody (712-005-153) was purchased from Jackson ImmunoResearch. Nuclease-free BSA (AB00445) was purchased from AmericanBIO. Amicon ultra-0.5 spin column (UFC510096) was purchased from Millipore. Illustra NAP-5 column (17085301) was purchased from GE Life Sciences. 8 well glass bottom chambered μ-slide (80827) was purchased from ibidi.

2. Methods

2.1. Design and synthesis of DNA nanostructure platform

Synthetic DNA origami nanostructures were designed and self-assembled as described previously[1]. Briefly, the 20 nm grid single-molecule platform was designed with the caDNAno software[2], and were based on a twist-corrected variant of the rectangular structure from

Rothemund 2006[3]. Eight staple strands were biotin-modified for surface fixation. Eight staple strands were extended with sequences complementary to the CNVK-bearing labelling strand (9 nt in length), and four corner staples were extended directly with DNA-PAINT docking sequences (9 nt in length), both with one thymine base spacer.

DNA origami 20 nm square grid structures were self-assembled in a one-pot annealing reaction with 50 ul total volume, containing 10 nM scaffold strand (m13mp18), 100 nM unmodified staple strands, 120 nM biotin-modified strands and 1 uM strands with DNA-PAINT extensions in DNA origami folding buffer. The solution was annealed with a thermal ramp cooling from 90˚C to 25˚C over the course of 3 hours. Self-assembled DNA origami structures were directly used for super-resolution imaging without gel purification.

2.2. Synthesis of CNVK-bearing and fluorophore-labelled oligonucleotide

Oligonucleotides carrying a 3-Cyanovinylcarbazole (CNVK) modified base were synthesized using standard phosphoramidite chemistry adapted from previous report[4] on an Expedite 8909 synthesizer (Perseptive Biosystems). Following synthesis, the CNVK oligonucleotide was cleaved from the column and deprotected for 8 hours in ammonium hydroxide at 55 C, then purified using Glen-Pak columns to remove truncated synthesis products. For the three-target labelling experiments, the product was then purified by reverse phase HPLC (0.1M TEAA, increasing ACN concentration from 5% to 50%). Product peak was identified with 260 nm (for DNA oligo) and 559 nm (for cy3b) absorption, and only the major fraction was collected, since the other minor peaks showed low crosslinking activity in the crosslinking efficiency assay.

Following purification, the CNVK strand was lyophilised, resuspended in water, and conjugated to a fluorescent dye with NHS-ester chemistry. Fluorophore-labelled oligonucleotide was synthesised in one-step NHS ester chemistry by mixing 20 ul of 1 mM amine-modified oligonucleotide, 2 ul 1 mM $NaHCO_3$ (pH 8.0) and 4 ul of 20 mg/ml cy3b NHS ester resuspended in DMSO. The reaction mix was shielded from light and incubated on shaker for at least 2 hours, and purified through NAP-5 column. Labelled-oligonucleotide was purified with another round of HPLC, the first (product) peak was collected then lyophilised before use.

Two CNVK-bearing sequences were designed and synthesised, AGv3 and E1v3. Crosslinking efficiency in Fig. 2, Supplementary Fig. 1 and 4 was tested with the AGv3 sequence. Blinking kinetics were measured for both sequences. All Action-PAINT experiments apart from two single-target labelling trials used the AGv3 sequence.

2.3. Characterisation of CNVK crosslinking efficiency and blinking kinetics

Characterisation of in-bulk CNVK crosslinking efficiency was performed with a handheld UV LED (LED-200, Electro-Lite Corporation). A droplet of mixed CNVK-bearing oligonucleotide and its complementary oligonucleotide strand in 1 uM was exposed to 1s illumination each, and the reaction solution was collected and assayed afterwards with denaturing acrylamide gel electrophoresis (10%) and staining with Sybr Gold. Crosslinking efficiency was calculated by comparing the intensity of crosslinked and non-crosslinked gel bands.

Characterisation of on-surface, single-molecule CNVK crosslinking efficiency was performed with synthetic DNA nanostructure standards (20 nm grid) and DNA-PAINT super-resolution microscopy as reported[1]. The nanostructures were designed with four fixed corner markers and eight CNVK reactive sites. During the crosslinking assay, the samples were exposed to 405 nm laser of 1, 3 or 15 discontinuous pulses of 1s illumination each, under typical TIRF microscopy conditions. Crosslinking was performed in the presence of 1 uM non-cy3b-labelled CNVK crosslinking strands, as well as 5 nM of cy3b-labelled CNVK crosslinking strands to help adjust the TIRF illumination angle. After crosslinking, the slide was washed several times with buffer before imaging with DNA-PAINT, and the number of successful crosslinking were counted within a collection (30-100) of nanostructures to calculate the crosslinking efficiency. Standard deviation of crosslinking efficiency was calculated assuming Poisson statistics.

CNVK-bearing labelling strand blinking kinetics were characterised with similar single-molecule platform as above. The blinking time trace from a DNA origami structure of the 20 nm grid (labelled with 8 CNVK reactive sites) were collected from DNA-PAINT super-resolution movie, and the characteristic blinking on-time and off-time were calculated by assuming a stochastic process for the blinking and fitting the on-time and off-time distribution to geometric distribution models, separately. A collection of these DNA origami structures was chosen and analysed together to obtain more accurate results.

2.4. Super-resolution fluorescence microscopy and DNA-PAINT

Single-molecule super-resolution fluorescence imaging was carried out on an inverted Nikon Eclipse Ti microscope (Nikon Instruments) with the Perfect Focus System, applying an objective-type TIRF configuration using a Nikon TIRF illuminator with an oil-immersion objective (CFI Apo TIRF 100x, numerical aperture NA 1.49). For single-colour experiments (pre-acquisition and post-acquisition), laser excitation with a 561 nm laser (for cy3b imaging, 200 mW, Coherent Sapphire) was passed through a clean-up filter (ZET561/10, Chroma Technology), coupled into the microscope objective using a beam splitter (ZT561rdc, Chroma Technology) and collected after emission filter (ET600/50m, Chroma Technology). For dual-colour experiments (real-time imaging and labelling sessions), 561 nm together with 405 nm laser (for UV crosslinking, 100 mW, Coherent Diode) were filtered through a multi-band filter cube (C-N Storm quad filter set, Nikon Instruments). Super-resolution movies were recorded without EM gain on an EMCCD camera (iXon X3 DU-897, Andor Technologies).

DNA-PAINT imaging for the pre-acquisition and post-acquisition samples was performed with protocol adapted from our previous work. In brief, biotin-labelled DNA nanostructures were immobilised on glass coverslips with BSA-biotin and biotin-streptavidin bridge, 5-10 nM of dye-labelled imager strands was used for the imaging sessions, in filtered imaging buffer B. Images were captured with 200 ms frame time (5 Hz). Each typical imaging session consisted of 10000 frames and lasted for ~30 min. Super-resolution image reconstruction and downstream analysis as well as kinetics measurement was performed in custom written MATLAB software.

2.5. Action-PAINT experimental procedure

The workflow of Action-PAINT super-resolution labelling experiment was conducted in three steps, and demonstrated on synthetic DNA nanostructure platform. Optimisation of imaging conditions was carried out in Nikon Elements software. Afterwards, custom written program in MATLAB (MathWorks) was used for camera recording, real-time image processing and crosslinking laser activation.

First, to "visualise", a pre-acquisition super-resolution image was recorded with DNA-PAINT with 200 ms acquisition time for 10000 frames, using 5 nM imager strands for drift markers and position markers and 10 nM imager strands for candidate labelling targets. The positions of all DNA nanostructure samples and drift markers as were then determined from the super-resolved image. Based on the results, one or more desired labelling target sites were manually selected, and a circular region of 20~40 nm in diameter was manually selected for each desired (include-ROI) and undesired labelling target (exclude-ROI). The positions of drift markers structures were automatically selected and imported to the real-time imaging and activation control software. Second, to "label", ~15 nM of CNVK-bearing labelling strands, together with 5 nM drift marker imager strands, was introduced into the flow chamber, replacing the previous imagers. After adjustment of TIRF illumination angle and drift correction matching, the real-time imaging and labelling session was controlled and recorded with custom software. Real-time labelling session was performed with 200 ms camera exposure and ~350 ms overall frame time (including real-time single-molecule fitting, super-resolution reconstruction and potential laser activation), and typically took 5000~10000 frames (30~60 min) to complete. Upon detection of on-target binding, a 405 nm crosslinking laser was activated for pulses spanning an integer number of frames, and allowed at a maximum threshold of 3 s per pulse. Finally, to "confirm", the CNVK-bearing labelling strand was exchanged again to regular DNA-PAINT imager strands of 10 nM for the reporter sequence as well as 5 nM for drift markers, and super-resolution image was captured with 200 ms frame time for 10000 frames for the post-acquisition image.

2.6. Real-time super-resolution reconstruction, drift correction and crosslinking laser activation

Real-time spot detection and super-resolution image analysis was performed with custom software written in MATLAB (MathWorks), adapted from previous report[1]. Efficient single-emitter localisation was performed with algorithm from Smith et al. 2010[5], without GPU acceleration. In practice, ~350 ms frame rate was achieved with 200 ms camera exposure time.

Afterwards, real-time drift correction was implemented with a collection of either origami drift markers (in the case of patterning on DNA nanostructures) or gold nanoparticles (in the case of microtubule *in situ* patterning) of previously known positions. At every frame, single-molecule localisations that matched drift marker positions were used to calculate the drift vector for the current frame, as well as updating the current position of the detected drift markers. An exponentially decay weighing factor was used to performed weighted average in drift vector calculation, with the optimal decay constant empirically determined based on characteristic off-time of the drift marker blinking kinetics.

Real-time UV activation was performed with 405 nm laser, in pulsed illumination of an integer number of frames per pulse. Activation of the 405 nm laser was performed by controlling the Nikon Elements software through the COM interface (Nikon Elements SDK, v4.4.1.728).

See Notes 3.1 for more details.

2.7. Preparation of oligo-labelled antibody

Oligo-labelled secondary antibody preparation was adapted from previous report[6]. Briefly, secondary antibody was first concentrated with Amicon 100kDa centrifugal filter to 2.5 mg/ml, and mixed with SMCC crosslinker (SM(PEG)2) to a final concentration of 2 mg/ml antibody and 0.05 mg/ml crosslinker in PBS, incubated at 4C for 3 hr and purified with Zeba 7k MWCO spin column. In parallel, thiol-modified oligo was reduced with 100 mM DTT, and purified with NAP-5 gravity column in ultrapure water.

The above maleimide-activated antibody was then mixed with reduced oligo at 1:15 eq. in PBS and incubated at 4C overnight. Final DNA-antibody conjugate was purified and concentrated with Amicon 100kDa centrifugal filter to 1.0 mg/ml and stored in 20 ul aliquots at -20C for future use.

2.8. Cell sample preparation for *in situ* microtubule labelling

BSC-1 cells were cultured with Eagle's minimum essential medium fortified with 10% FBS with penicillin and streptomycin and were incubated at 37 °C with 5% CO2. Cells were seeded into 8-well ibidi glass bottom chambers and grown to 50-60% confluency before fixation.

Microtubules were immunostained with the following protocol: washing in PBS, fixation with 4% paraformaldehyde (PFA) for 45 min, washing in PBS, quenching with 100 mM NH4Cl for 15 min, washing in PBS, permeabilisation and blocking with 2% BSA + 0.1% Triton X-100 in PBS for 3 x 10 min, staining with rat anti-alpha-tubulin antibody (1:50 dilution) in 2% BSA + 0.1% Trion X-100 in PBS at 4C overnight, washing with 2% BSA + 0.1% Triton X-100 in PBS for 3 x 10 min, staining with oligo-conjugated donkey anti-rat secondary antibody (1:50 dilution) and 0.2 mg/ml sheared salmon sperm, 2% BSA, 0.1% Triton X-100 and 4 mM EDTA in PBS at RT for 1 hr, washing with 0.1% Triton X-100 in PBS for 10 min, washing in PBS for 2 x 10 min, post-fixation with 5 mM BS(PEG)5 for 30 min, washing in PBS, quenching with 100 mM NH4Cl for 5 min, washing in PBS. Fixed cell samples were then kept in PBS at 4C before use.

2.9. Localisation based analysis for microtubule labelling

For super-resolution patterning experiments on fixed microtubule samples, due to the unknown multiplicity of target sites within the include-ROI and exclude-ROI areas, it is difficult to quantify the degree of specific labelling using the same counting method, as in the case for isolated single-site patterning on DNA nanostructures. We therefore employed a different, localisation-based method for crosslinking efficiency and specificity assay, as described below.

We first measured the total number of single-molecule localisations observed in the pre-acquisition and post-acquisition DNA-PAINT movie stacks, respectively. These localisation counts (normalised by movie length and imager concentration) provide an effective measure of the total number of oligo targets or labels in the respective ROI regions. Then, crosslinking efficiency was calculated from the ratio between post- and pre-image localisation counts, and crosslinking specificity (fold enrichment) was further calculated from the ratio between the crosslinking efficiency in include- and exclude-ROIs. To offset the effect on crosslinking efficiency and specificity calculations from labelling close to the ROI boundaries (likely due to lack of overall achievable labelling resolution), we used edge-buffered ROI areas for these calculations (increasing the include-ROIs and simultaneously shrinking the exclude-ROIs by 20 nm on each side). See Supplementary Notes 1.3 for more details.

2.10. Simulation for Action-PAINT experiments

To better understand how various parameters affect the overall success rate of Action-PAINT, we performed *in silico* simulations of Action-PAINT experiments on a multi-target sample, similar to the experiments performed on DNA origami grids. We simulated the stochastic binding of CNVK imager and laser-induced crosslinking that follows (both desired crosslinking by the 405 nm laser and non-specific crosslinking by the 561 nm imaging laser). The parameters we simulated and compared include the characteristic binding on-time, off-time, number of include- and exclude- ROIs and imaging session length.

We estimated the per-frame crosslinking rate to be 0.18, from the 45% crosslinking efficiency after a single 1s 405nm laser exposure (Fig. 2b), and the effective per-frame background crosslinking rate to be 0.008 and 0.012 for the 2-choose-1 and 6-choose-3 experiments, respectively. To calculate the background crosslinking rates, we measured the overall background crosslinking rates (11% and 15%) and assumed that target is bound by a CNVK imager for an average of 15 frames during an entire imaging session. We incorporated similar stop criteria as in the experiments: (1) An include ROI should receive at least 1 frame of UV exposure (due to the 1 frame delay in recording and UV activation, a 1 frame UV exposure will require at least a 2 frame binding event) and (2) no further blinking is observed within the include-ROI after a set monitoring time window of 1000 or 2000 frames (roughly 5 or 10 minutes, for 2-choose-1 and 6-choose-3 experiments, respectively). If the above criteria is not met after a set imaging session length (5000-10000 frames), the experiment is stopped. An experiment was considered successful only if all of the include-ROIs none of the exclude-ROIs are labelled.

We note that a few experimental effects were not considered in the simulation, including drift and localisation error, damaged or misbehaving origami nanostructures, effect of crosslinking laser power control, TIRF angle and the control limit of up to 3 s of illumination per target, and the effect of photo-induced crosslinking reversal (which is potentially limiting for multi-point labelling experiments, however the reversal rate was difficult to estimate and simulate faithfully). These missing aspects likely explains the difference between the simulated and experimental overall success rates.

3. Notes

3.1. Notes on Action-PAINT control software and real-time analysis

3.1.1. General control software design

The real-time Action-PAINT control and analysis software GUI was custom developed in MATLAB (MathWorks), and consists of four components in general, (i) camera and microscope control and data acquisition, (ii) efficient real-time single-molecule fitting, (iii) high-precision real-time stage drift correction, and (iv) Action-PAINT control logic, as well as various logging and output activities (Supplementary Fig. 5).

The real-time spot detection and super-resolution image analysis was adapted from our previous work. Real-time camera and laser control and data acquisition was performed with a combination of direct Andor APIs and Nikon Elements COM interface. Efficient single-emitter localisation was performed with algorithm adapted from Smith et al. 2010[5], without GPU acceleration. In practice, ~350 ms overall frame rate was achieved with 200 ms camera exposure time and optimised analysis routine. The high-precision stage drift correction algorithm and activating laser control was specifically designed and implemented for real-time operation in Action-PAINT.

3.1.2. Real-time high-precision stage drift correction

We implemented a real-time, high-precision stage drift correction strategy adapted from our previous work using DNA nanostructures as drift markers[1]. Here, we used the 20 nm square grid nanostructures and treated each nanostructure as one fiducial markers without considering its internal structures (i.e. without implementing the Templated Drift Correction algorithm).

Compared with our previous off-line drift correction algorithm, there are two difficulties for on-line (i.e. real-time) drift correction: (i) only the history positions of each blinking target are known at the time of correction, therefore methods based on interpolation between neighbouring events in blinking time trace cannot be implemented, (ii) although the locations of drift markers could be measured ahead of time (during pre-acquisition), the stage drift in between the pre-acquisition and actual experiment is unknown.

In order to make up for the loss of possibility of interpolation between blinking events, we implemented an exponential time-decay weighted averaging method, such that each blinking event contribute to the drift correction of a number of frames, and more recent blinking events carry higher weight (higher "confidence"). The optimal decay constant was determined based on characteristic off-time of the drift marker blinking kinetics, and empirically works best in the range of 5-20 frames. This strategy effectively solves the difficulty (i) above by allowing an effectively higher number of blinking events and drift markers be used for each frame, therefore giving higher accuracy drift correction, as well as higher robustness against noise-induced mis-correction.

To solve difficulty (ii), we then implemented a cross-correlation based matching method, that is used to find the "missing" drift during the experimenter operation time (i.e. data analysis, buffer exchange) between the pre-acquisition and real-time Action-PAINT imaging sessions. In details, the blinking events from any real-time imaging frame is matched against the pre-determined locations of all drift markers by computing the cross-correlation matrix. Real-time Action-PAINT will only start if a sharp peak is identified, indicating a successful matching process.

During real-time Action-PAINT session, the number of blinking events that match the known drift marker locations is used as a quality control for drift correction quality. If the number of matched localisation remains above a certain set threshold (typically 10~15), the system is considered to remain "drift locked", and crosslinking laser could be activated; otherwise, the system is considered "drifting", no drift correction is computed from the current frame, and the crosslinking laser is blocked.

We estimated our experimentally achieved drift correction accuracy by measuring FWHM (full-width at half-maximum) of single-spot targets (an ensemble of overlapped targets). Using this assay, we report ~5 nm (r.m.s.) of remaining drift achieved with our real-time drift correction, and in comparison, ~4 nm (r.m.s.) with post-analysis drift correction (Supplementary Fig. 6). Together with ~10,000 photons per average localisation event with 2.7 nm localisation precision, taken under typical Action-PAINT compatible conditions, we observed a typical frame-to-frame stage drift of ~1 nm (r.m.s.), and obtained 12~15 nm imaging resolution (FWHM), as well as resolved individual grid points on a 20 nm grid structure from each other (Supplementary Fig. 6).

3.1.3. Action-PAINT crosslinking laser control logic

The general principle of Action-PAINT crosslinking laser control is to synchronise on-target binding of the CNVK labelling strand and crosslinking illumination. Therefore, a single-molecule localisation that is detected within the include-ROI region triggers the activation of the crosslinking laser, subject to the following extra conditions: (i) the localisation passes general quality control (minimum photon count threshold, localisation precision threshold), (ii) at least two frames of continuous blinking have been detected, and (iii) a maximum dosage of crosslinking illumination (3 s) can be conducted on any single blinking event, in order to prevent undesired adverse effects, such as crosslinking reversal by the same illumination. Furthermore, (iv) any apparent blinking event that drifts outside of the include-ROI region (due to background noise and fitting error) or that visits one of the exclude-ROI regions is excluded from triggering crosslinking laser.

The detailed Action-PAINT decision and control logic is detailed in a flow diagram shown in Supplementary Fig. 7. We implemented the above requirements with a few control flags, detailed as follows.

- "on_limit": for monitoring the total crosslinking laser dosage for any single continuous blinking event.
- "streak_flag": for detection of continuous 2-frame localisations
- "laser_block": for detection of blinking events that drifts outside of include-ROI regions (due to background noise and fitting error) or that visits one of the exclude-ROI regions

Note that in the above, as well as other places in the paper, we use "localisation" to refer to the super-resolved centre position (from fitting a two-dimension Gaussian to the point spread function) of a single camera frame, whereas we use "blinking event" to refer to a physical instance of a CNVK labelling strand hybridising onto the target strand. Therefore, one "blinking event" typically consists of a few "localisations", from adjacent camera frames.

3.1.4. Stopping criteria for in situ microtubule labelling

For the in situ microtubule labelling experiments, due to the unknown multiplicity of target sites within the include-ROI area, it is difficult to assay the degree of crosslinking during the real-time labelling session using the blinking kinetics analysis as in the case for isolated single-site patterning on DNA nanostructure. We therefore employed a different set of stopping criteria, based on the total dose of crosslinking illumination received on the target sites: (i) each target ROI should receive at least three separate crosslinking illuminations, (ii) ideally, at least one of the illuminations should last for two imaging frames or longer, (iii) the total number of frames for the real-time labelling session should not exceed a set limit (3000 frames). In practice, it is difficult to require all three criteria to be met simultaneously for all experiments, we therefore set (i) and (iii) to be met at all times, and allowed an extension of the labelling session for an additional ~500 frames in the case (ii) is not met. In the edge case where only criteria (i) is met after the imaging session has exceeded 2500 frames, thereby excluding the possibility of meeting criteria (ii) and (iii) within the next 500 frames, the imaging session is stopped regardless and is still considered to be a valid Action-PAINT experiment.

3.2. Notes on factors affecting crosslinking efficiency and success rate

We hypothesised that the current Action-PAINT crosslinking efficiency and success rate could be limited by a few factors as described below: (i) occasional mis-localisation during the real-time imaging analysis, (ii) unintended crosslinking due to dark fluorophores, (iii) background crosslinking by the imaging laser, (iv) absence of on-target binding of CNVK labelling strands, and (v) crosslinking reversal of previously crosslinked strands. Of these, (i) through (iii) mostly contributes to mis-labelling of off-target sites, while (iv) and (v) mostly contributes of missed on-target labelling.

3.2.1. Off-target mis-labelling from mis-localisation, dark fluorophores, and background crosslinking

Intuitively, occasional mis-localisation of CNVK labelling strand binding events could contribute to off-target mis-labelling. The reason for the mis-localisation could be a combination of a higher imaging background during the Action-PAINT workflow (due to the requirement of high blinking rate for efficient crosslinking, and a mixture of CNVK labelling strands, corner marker and drift marker imaging strands), and occasional failure of real-time drift correction algorithm (due to the lack of interpolation capability, especially during fast stage drift). However, mis-localisation induced mis-labelling has only been occasionally observed (in the three-target labelling experiments only), and does not explain the majority of off-target labelling cases.

From offline analysis of the time traces for the two instances of off-target labelling during the single-target labelling experiments, we noticed that all bindings to the off-targets (exclude-ROI regions) were correctly localised and did not trigger the 405 nm laser. It is therefore not mis-localisation that resulted in these off-target labelling. We then hypothesised that off-target labelling could also result from either dark fluorophore (non-fluorescent species or photobleached during the sample preparation), or imaging laser (561 nm) induced crosslinking. The effect of dark fluorophores is difficult to characterise. However, we conducted control experiments on the DNA grids in the presence of CNVK labelling strands and under typical 561 nm laser illumination only. The results showed that a continuous 30 min illumination of 561 nm laser under typical TIRF imaging conditions (0.5~1 kW/cm^2) can introduce a ~10% background crosslinking rate. This effect could be further exacerbated during the three-target labelling experiments, since a longer imaging and labelling session is typically required as compared to the single-target case.

3.2.2. Failed on-target labelling from damaged labelling target and crosslinking reversal

Two major failure modes were observed for failed on-target labelling during our Action-PAINT experiments. The first failure mode concerns some labelling target sites that were never visited by a CNVK labelling strand during the Action-PAINT labelling session, although pre-acquisition images clearly showed the presence of these labelling target sites. We hypothesised that these labelling target sites could have been damaged during consecutive imaging sessions and buffer exchange, as our previous experiments (data not shown) have indicated that repeated rounds of buffer exchange and super-resolution imaging session could damage the DNA nanostructures and result in loss of grid points (and occasionally damage of the overall nanostructure) over time.

Another effect that could limit our current on-target labelling efficiency is potential photo-induced crosslinking reversal, that liberates the CNVK-bearing strand from a previously crosslinked target strand. Crosslinking reversal for CNVK has been observed and reported previously, under 365 nm illumination[7]. In our case, successful on-target crosslinking is typically indicated by a relatively long blinking event (since the dye-labelled CNVK-bearing strand is fixed at the target site and remains bright until photobleached) followed by a permanent darkness at the target site (since the target site is now inaccessible to other CNVK strands). We typically monitor a candidate crosslinked target for 5-10 minutes after triggering the 405 nm laser illumination to determine if the docking site is indeed no longer accessible. However, in some instances docking sites that appeared to have been crosslinked to a CNVK imager will be re-visited by another imager after the 5~10 min observation window. Similar to above, this effect could be further exacerbated during the three-target labelling experiments, since we do not expect all target sites to be successfully labelled at the same time, and a longer imaging and labelling session could result in a higher post-crosslinking illumination dosage, and thus a higher chance of crosslinking reversal.

3.3. Notes on edge-buffered ROIs for crosslinking efficiency and specificity calculation

We observed quite a number of labels either right at the edge of the include-ROI or at the edge of (and inside) exclude-ROIs, likely due to the small target ROI area and the limitation in overall achievable labelling resolution (~20 nm, from combined effect of localisation precision, drift correction residual, and potential antibody and sample movement). To offset this effect in our measurements, we included an edge buffer to the ROI areas during the above analysis. Specifically, we enlarged include-ROIs by 20 nm on each side, and simultaneously shrinked exclude-ROIs by the same amount (as shown in Fig. 4b, last row and Supplementary Fig. 12a, last row), and calculated the pre- and post-image localisation counts according to the adjusted ROIs.

We note that such operation is valid since it is always possible to set the include-ROI area in the real-time laser control program to be smaller than the actually intended target area to achieve the same end result. Indeed, we observed higher crosslinking efficiency and specificity values calculated from these buffered ROI areas (see comparison in Supplementary Fig. 13), which also provided indirect support that these off-edge labels are indeed specific crosslinking events but just mis-located due to limited overall resolution.

3.4. Notes on statistics and reproducibility

Single-point labelling experiment (with 70 nm selectivity) was performed a total of 33 times. Out of which 22 were assayed for labelling efficiencies (with post-acquisition), and the rest 11 were aborted half-way. Out of these 22 experiments, 11 showed desired on-target labelling without off-target labels, 9 showed no labelling either on-target or off-target, and 2 showed opposite labelling (in exclude-ROI instead). Fig. 2b and Supplementary Fig. 8 show five representative successful labelling experiments, and Supplementary Fig. 9 shows five representative unsuccessful cases.

Multi-point labelling (6-choose-3) experiment (with 30 nm selectivity) was performed a total of 84 times. Out of which 62 were assayed for labelling efficiencies (with post-acquisition), and the rest 22 were aborted half-way. Out of these 62 experiments, 17 showed all 3 on-target labels, 26 showed 2 of 3, 18 showed 1 of 3, and only 1 showed no on-target labels; on the other hand, 42 out of 62 showed no off-target labels, 16 showed 1, 3 showed 2, and only 1 showed three off-target labels. Overall, 10 showed complete success (3 on-target, 0 off-target). Of all tests, we focused most of our time (N=70) on one pattern of intermediate difficulty (middle column in Fig. 3c); for the rest, we repeated each test a few times. The total number of tests performed for each pattern (in the order as shown in Fig. 3c) are N = 1, 4, 70, 5, 4, respectively. There was no sign showing this pattern gives particularly high labelling success rate compared to others (6/70 overall success for this pattern vs 4/14 overall success aggregated over all other patterns). Fig. 3c and Supplementary Fig. 10 show five representative successful labelling experiments, one for each distinct pattern, and Supplementary Fig. 11 shows five representative unsuccessful cases.

Two-point labelling experiment on fixed microtubule samples (with 40 nm selectivity) was performed with a total of 8 times (after labelling protocol optimisation). Out of these experiments (N=4, 2, 2 for three different spacings of 160 nm, 320 nm, 480 nm, respectively), all samples were assayed with post-acquisition, as shown in Fig. 4c. Out of these experiments, 7 were counted, and one was excluded due to suspected sample movement. Out of the 7 counted

experiments, 4 showed both on-target labels, and 3 showed one on-target label; on the other hand, 3 showed 0 out of 3 off-target label, 3 showed 1, and 1 showed 2. Overall, 2 showed complete success (2 on-target, 0 off-target). Fig. 4c shows three representative successful labelling experiments, one for each different spacing, and Supplementary Fig. 13 shows three representative unsuccessful cases.

References

1. Dai, M., Jungmann, R. & Yin, P. Optical imaging of individual biomolecules in densely packed clusters. *Nat Nanotechnol* **11,** 798–807 (2016).

2. Douglas, S. *et al.* Rapid prototyping of 3D DNA-origami shapes with caDNAno. *Nucleic acids research* **37,** 5001–6 (2009).

3. Rothemund, P. W. Folding DNA to create nanoscale shapes and patterns. *Nature* **440,** 297–302 (2006).

4. Yoshimura, Y. & Fujimoto, K. Ultrafast Reversible Photo-Cross-Linking Reaction: Toward in Situ DNA Manipulation. *Org Lett* **10,** 3227–30 (2008).

5. Smith, C. S., Joseph, N., Rieger, B. & Lidke, K. A. Fast, single-molecule localization that achieves theoretically minimum uncertainty. *Nat Methods* **7,** nmeth.1449 (2010).

6. Agasti, S. S. *et al.* DNA-barcoded labeling probes for highly multiplexed Exchange-PAINT imaging. *Chemical Science* **8,** 3080–3091 (2017).

7. Vieregg, J. R., Nelson, H. M., oltz, B. & Pierce, N. A. Selective nucleic acid capture with shielded covalent probes. *Journal of the American Chemical Society* **135,** 9691–9 (2013).

1. Figures

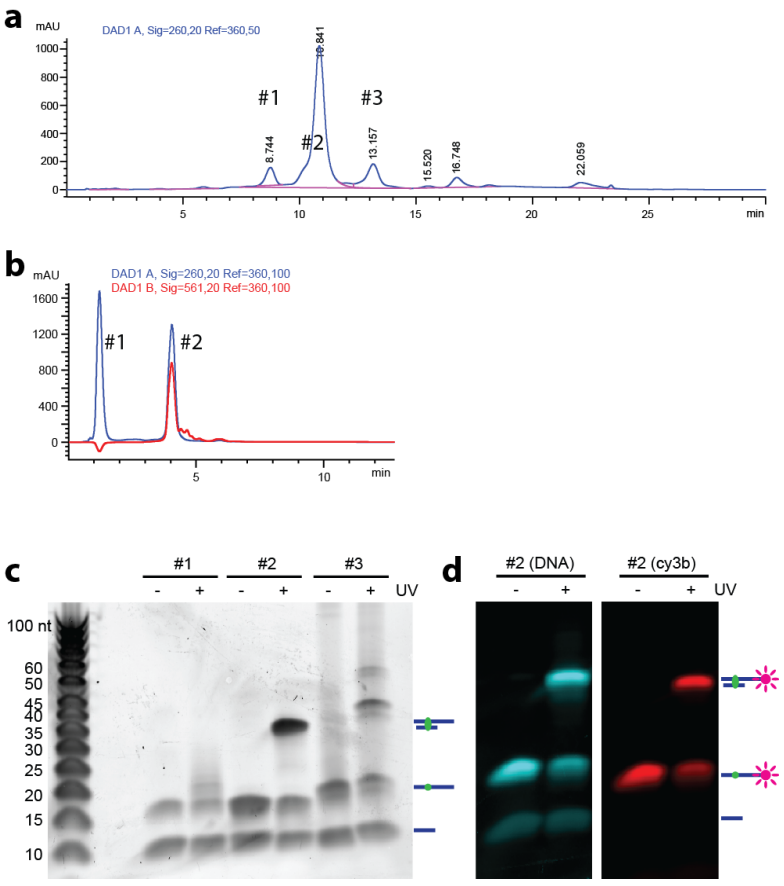

Supplementary Fig. 1 Synthesis of CNVK-bearing imager strands
(**a**) HPLC trace and fractions of synthesised CNVK-bearing crosslinking strands. (**b**) HPLC trace and fractions of synthesised cy3b-labelled CNVK-bearing imager strands. (**c**) Crosslinking assay of the three HPLC fractions from (a) on a denaturing PAGE gel. (**d**) Crosslinking assay of the second HPLC fraction from (b) on a denaturing PAGE gel, imaged for both DNA oligo and cy3b dye. Both crosslinking assay was performed with 1s illumination of 365 nm handheld UV device. Chemical synthesis of CNVK strands listed in Table 4A, HPLC purification, and crosslinking tests were performed N=6 independent times. See also Supplementary Methods 2.2 for more details.

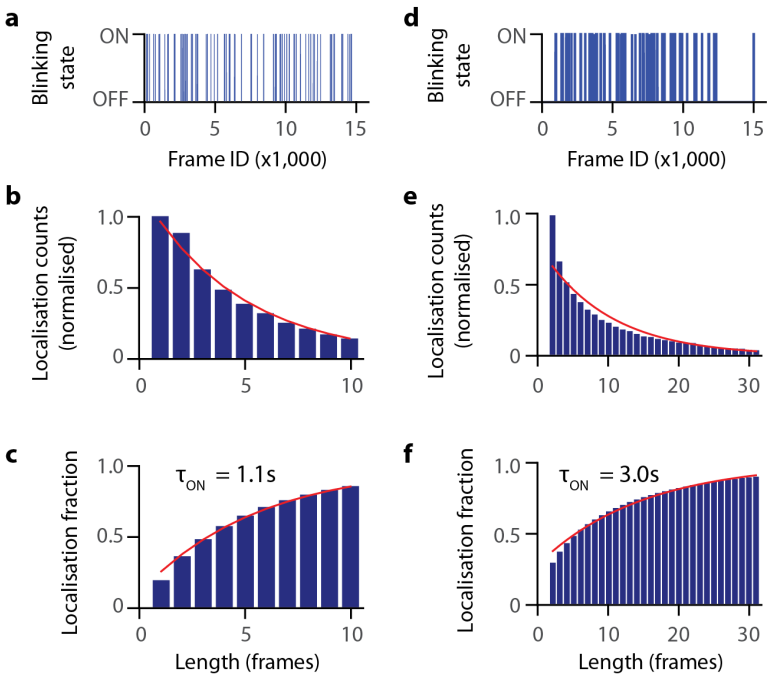

Supplementary Fig. 2 Single-molecule blinking kinetics test for CNVK-bearing strands for sequence AGv3 (**a,b,c**) and E1v3 (**d,e,f**). (**a,d**) Representative blinking time trace on a DNA origami test structure. (**b,e**) Histogram of single-molecule blinking event lengths and fitting to stochastic process model, measured in stochastic process model. See also Supplementary Methods 2.3 and 2.4 for more details.

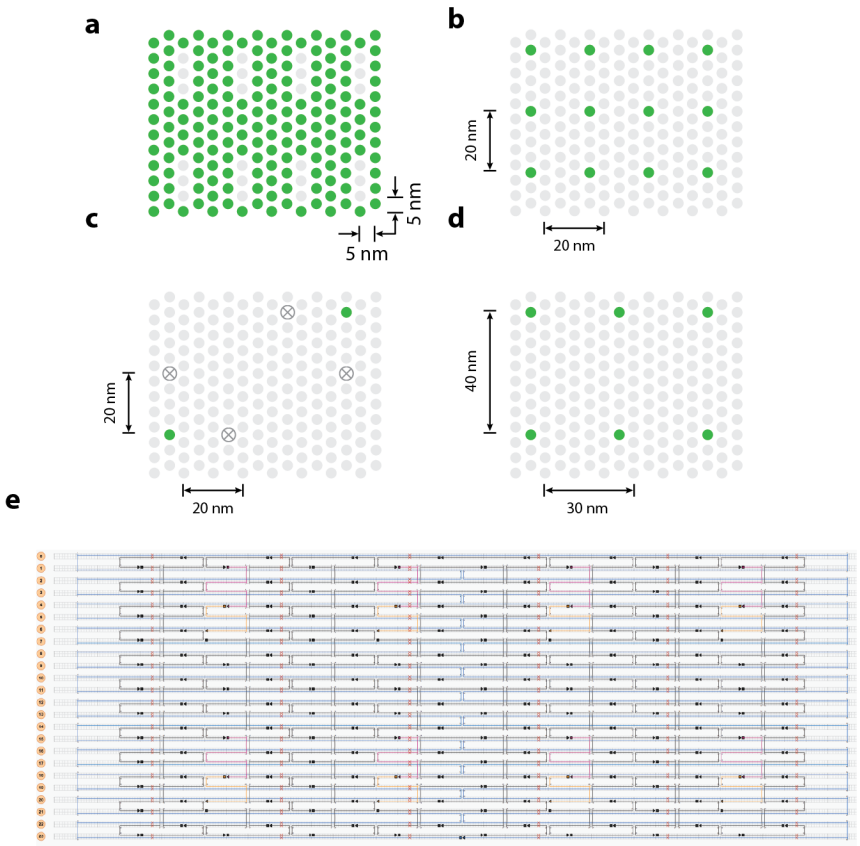

Supplementary Fig. 3 DNA origami nanostructure design strand diagram and schematics
(**a-e**) Strand diagram and design schematics of the twist-corrected rectangular DNA origami nanostructure used in this paper. (**a**) Simplified design schematic for a rectangle shaped DNA origami nanostructure in (e), where each staple is represented by a dot. Green dots indicate staple strands that can be extended with DNA-PAINT docking or labelling strands, grey dots indicate staple strands that cannot be extended for DNA-PAINT imaging. (**b**) Simplified design schematic for the 20 nm square grid structure, used as drift correction markers. (**c**) Simplified design schematic for the 70 nm separation, single-target labelling test. (**d**) Simplified design schematic for the 30 nm separation, three-target pattern labelling test. (**e**) Detailed strand diagram for the unmodified origami rectangle, showing twist-corrected DNA origami design. Thin blue lines: circular scaffold strand. Black lines: unmodified staple strands. Orange and crimson lines: strands with biotin extension for surface fixation, and strands with modified wiring pattern to accommodate those orange ones. Red crosses: positions of deleted bases. See also Supplementary Methods 2.1 for more details.

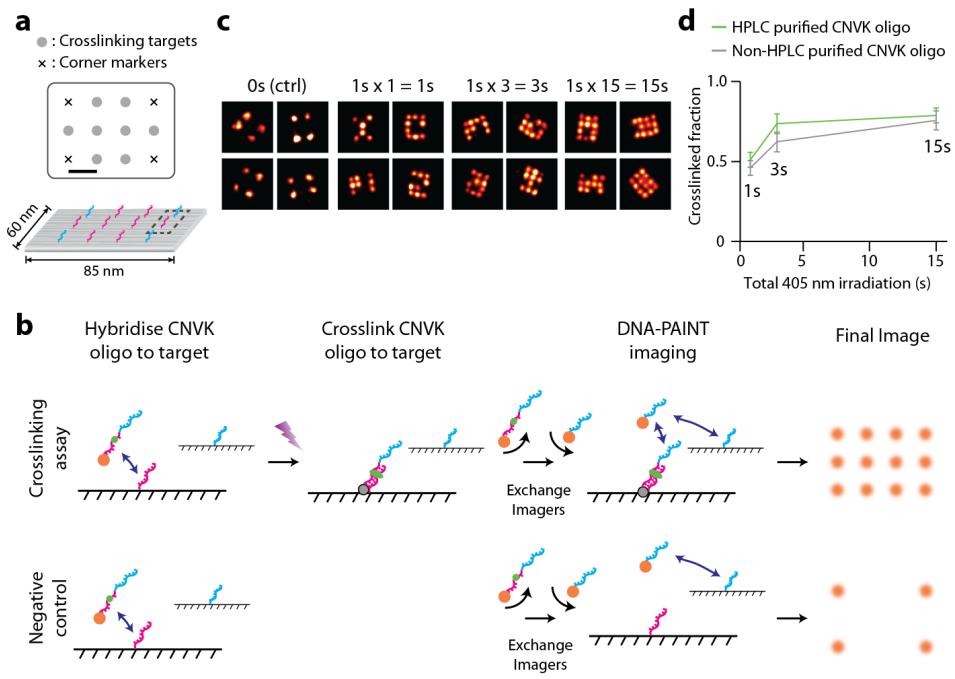

Supplementary Fig. 4 Single-molecule CNVK crosslinking efficiency test
(**a**) DNA nanostructure grid design for single-molecule CNVK crosslinking assay. (**b**) Schematics showing workflow of single-molecule CNVK crosslinking assay. Top, crosslinking assay, bottom, negative control. A DNA grid that is fully cross linked will present all 8 internal sites and the 4 reference sites in a post crosslinking DNA-PAINT super-resolution image. (**c**) Representative images of DNA grids after 0, 1, 3 or 15 sec of cumulative 405 nm laser exposure. (**d**) Crosslinking efficiency measured as a function of 405 nm UV irradiation. Error bars represent uncertainty assuming Poisson statistics. Error bars represent Poisson counting uncertainty. For non-HPLC purified samples, total number of grids counted: 80, 53, 48, respectively, each having 8 binding sites; number of labelled targets: 299, 262, 289, respectively. For HPLC purified samples, total number of grids counted: 103, 60, 82, respectively, each having 8 binding sites; number of labelled targets: 419, 349, 510, respectively. Scale bars 20 nm. See also Supplementary Methods 2.1 and 2.3 for more details.

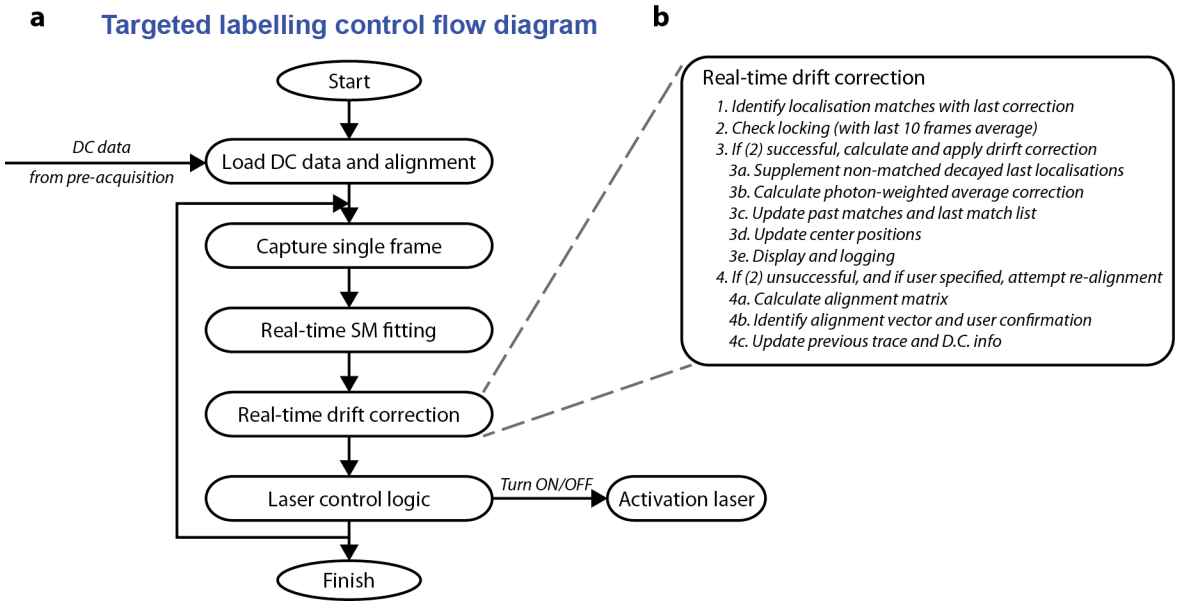

Supplementary Fig. 5 High-level software control flow diagram for real-time single-molecule labelling session (**a**) and algorithm outline for high-accuracy real-time drift correction (**b**). DC, drift correction, SM, single molecule. See also Supplementary Methods 2.6 and Notes 3.1.2 for more details.

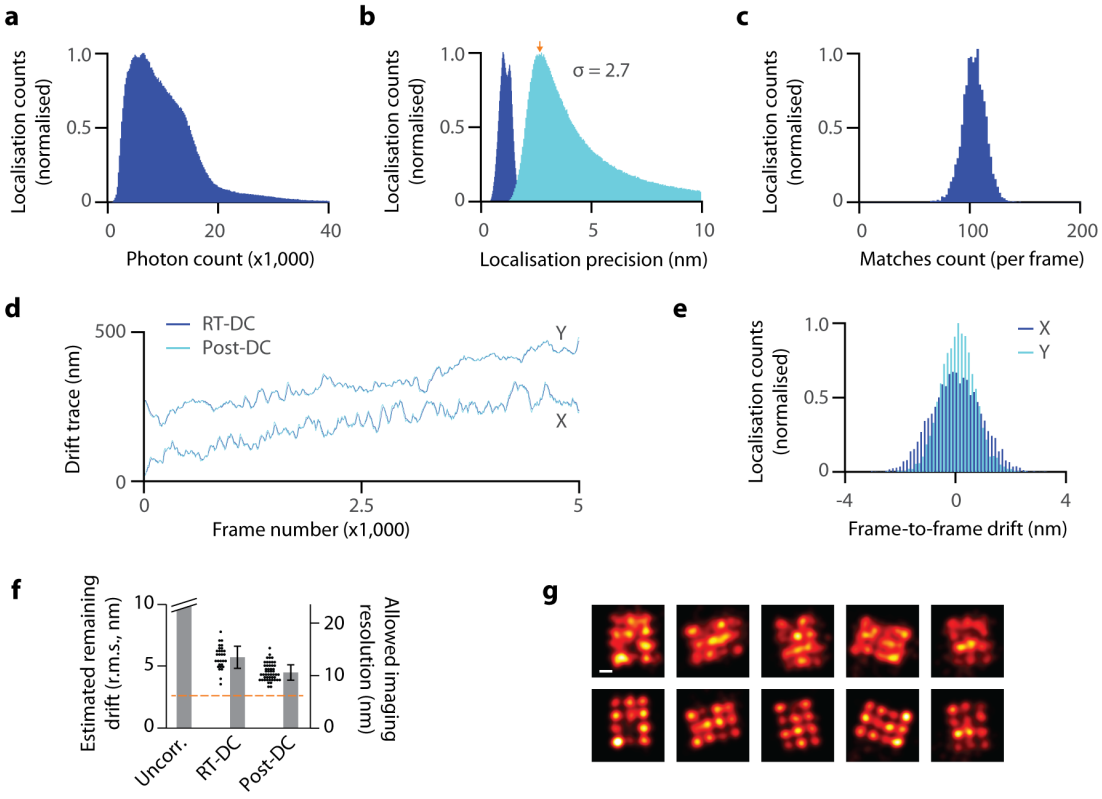

Supplementary Fig. 6 Real-time drift correction performance characterisation.
(**a**) Histogram of photon count per localisation. (**b**) Histogram of fitting reported uncertainty (FRU, in blue) and theoretical localisation precision limit (in cyan). (**c**) Histogram of number of matched localisations per frame used for real-time drift correction. (**d**) Comparison of real-time drift correction (blue) and post-processed drift correction (cyan) time traces. Traces for Y are manually shifted. (**e**) Distribution of frame-to-frame drift in X and Y. (**f**) Comparison of estimated remaining drift (in r.m.s.) and allowed imaging resolution for uncorrected, real-time corrected and post-processing corrected images. For RT-DC and Post-DC samples, N=29 and N=49 single-molecule targets were analysed, error bars indicate mean ± standard deviation, dot plots are offset to the left for visual clarity. (**g**) Representative 20 nm grid samples with real-time (top) and post-processed (bottom) drift correction. N=3 independent experiments were repeated with similar results. Scale bar, 20 nm. See also Supplementary Methods 2.6 for more details.

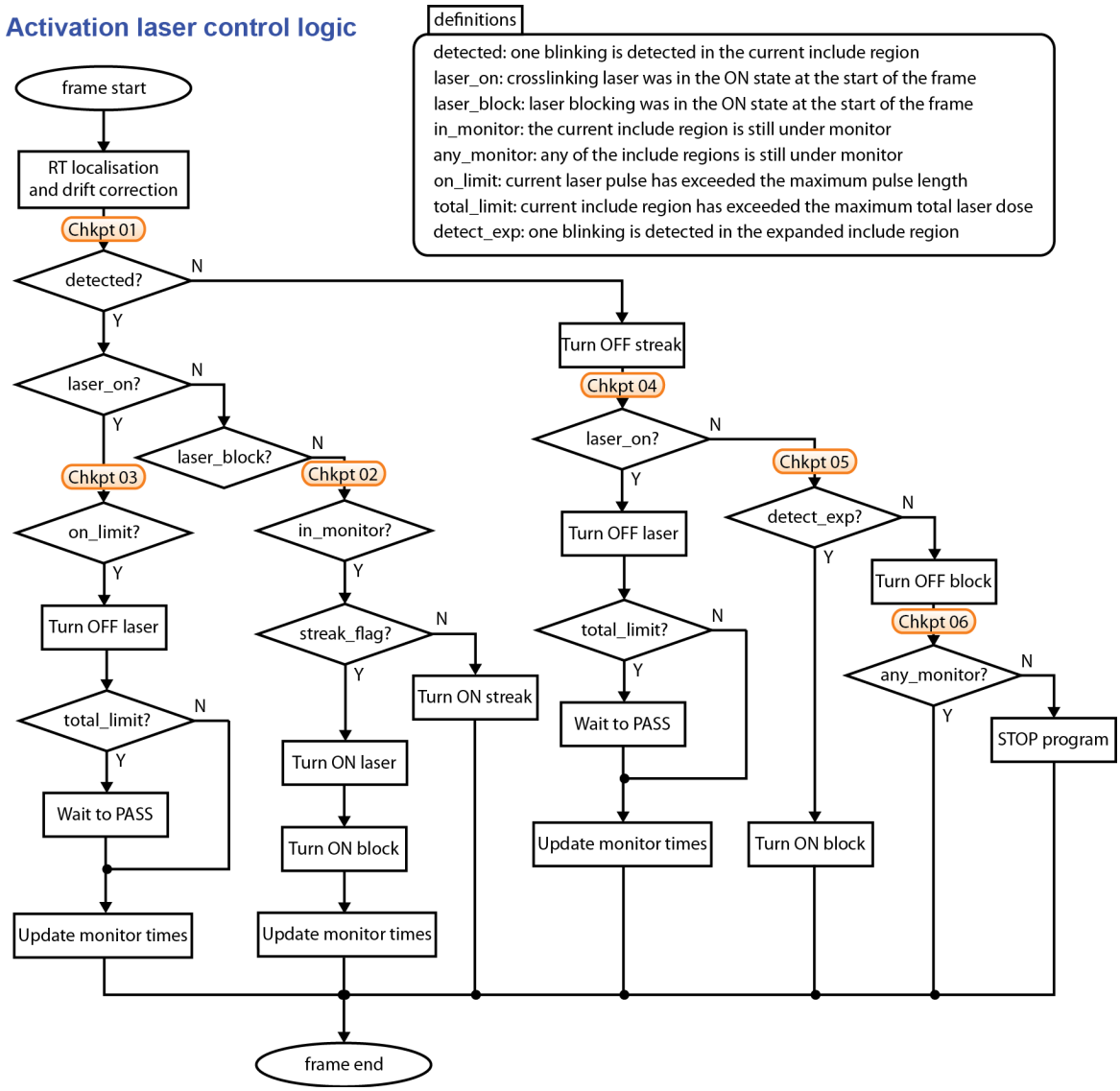

Supplementary Fig. 7 Software control logic flow diagram for crosslinking laser activation. See also Supplementary Methods 2.6 and Notes 3.1.3 for more details.

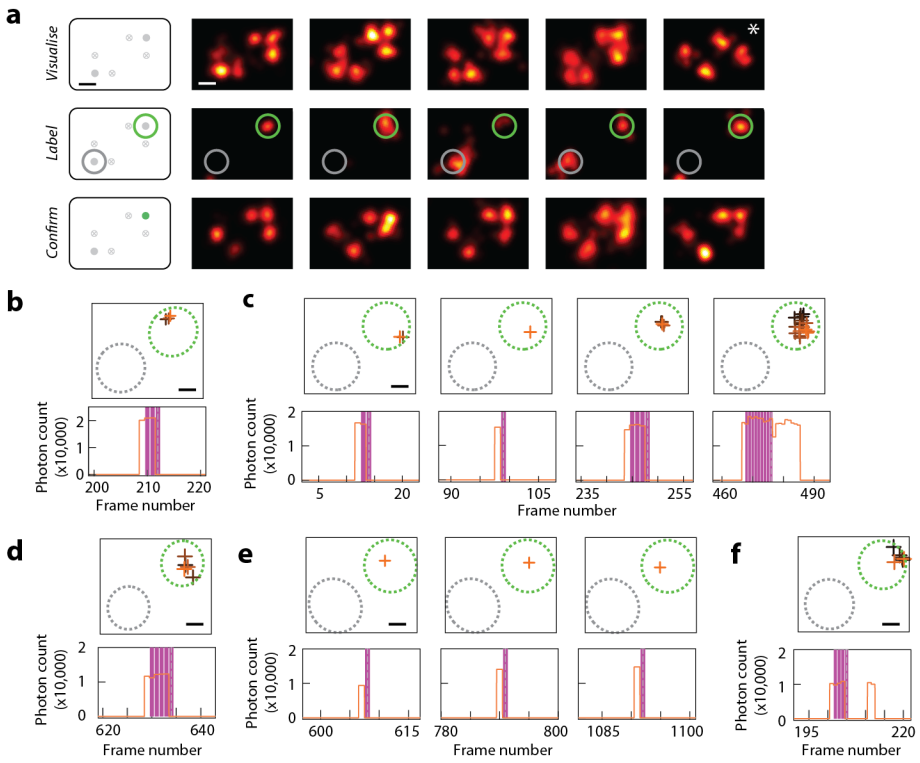

Supplementary Fig. 8 Representative examples of successful Action-PAINT single-molecule labelling. (**a**) Schematics and super-resolution images of representative examples of successful labelling trials, at each stage of the experiment. Left column, schematics, right columns, super-resolution images. Top row, pre-acquisition images ("visualise", image with asterisk was taken without candidate targets), middle row, real-time labelling session images ("label"), bottom row, post-acquisition images ("confirm"). In schematics, grey circles with a cross in schematics indicate markers, grey and green solid dots indicate markers, candidate (unlabelled) and successfully labelled target sites, respectively. Green and grey circles overlaid on both schematics and super-resolution images indicate desired and undesired target sites, respectively. Super-resolution images of real-time labelling session were normalised differently to show the blinking spots. (**b-f**) Real-time blinking and laser activation traces for the samples in (a). Blinking events are separated into different panels, for each detected blinking event, XY (top) and time traces (bottom) are shown. XY traces are colour-coded by time (from black to orange) and overlaid with include- (green, dotted circle) and exclude- (red, dotted circle) ROIs; time traces show detected photon count per single-molecule localisation (orange), overlaid with laser illumination (magenta) and monitor events (dashed line). All scale bars, 20 nm. See also Supplementary Methods 2.5 for more details, and Supplementary Notes 3.4 for discussion regarding statistics and reproducibility.

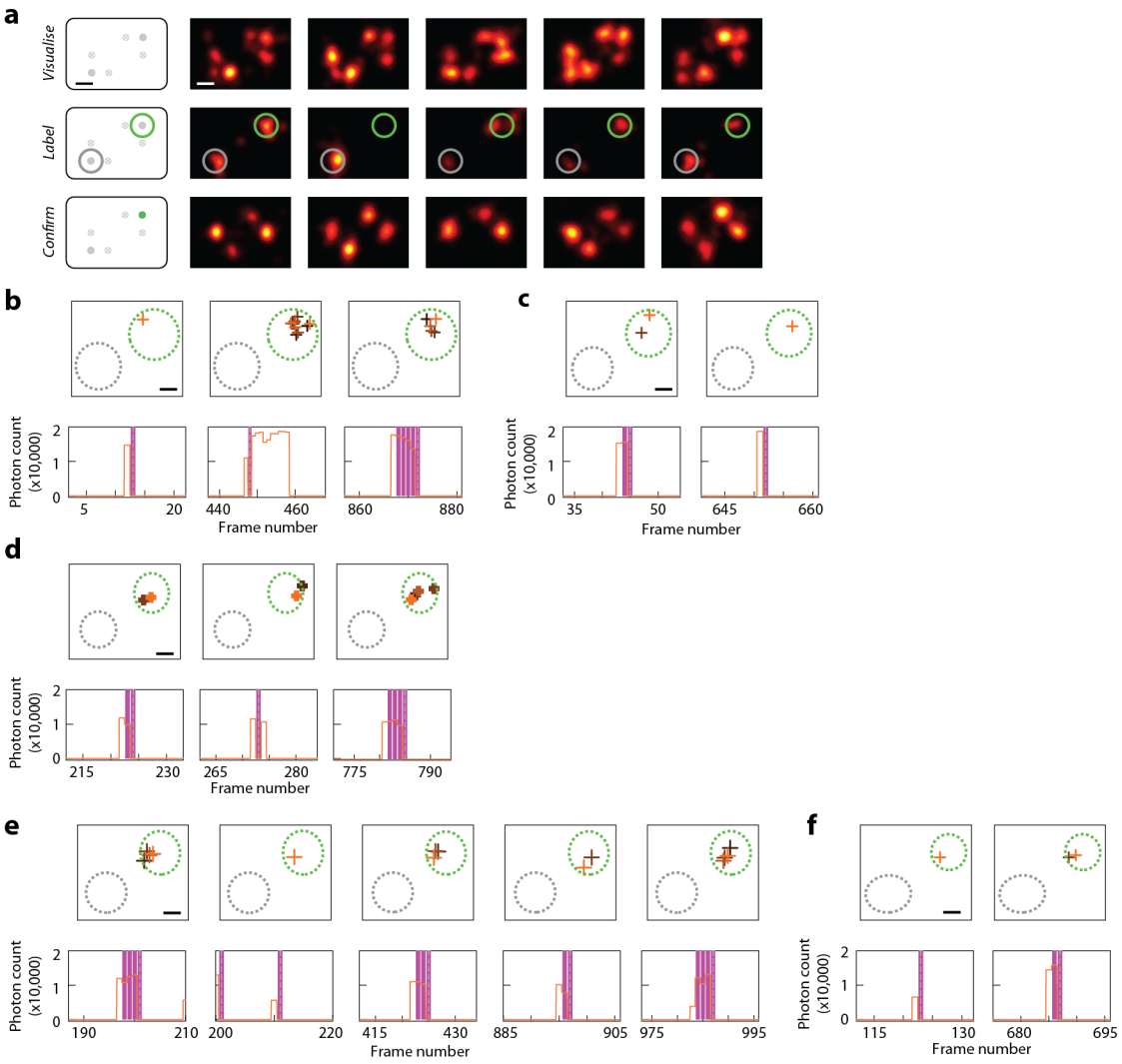

Supplementary Fig. 9 Representative examples of failed Action-PAINT single-molecule labelling. (**a**) Schematics and super-resolution images of representative examples of successful labelling trials, at each stage of the experiment. Left column, schematics, right columns, super-resolution images. Top row, pre-acquisition images ("visualise", image with asterisk was taken without candidate targets), middle row, real-time labelling session images ("label"), bottom row, post-acquisition images ("confirm"). In schematics, grey circles with a cross in schematics indicate markers, grey and green solid dots indicate markers, candidate (unlabelled) and successfully labelled target sites, respectively. Green and grey circles overlaid on both schematics and super-resolution images indicate desired and undesired target sites, respectively. Super-resolution images of real-time labelling session were normalised differently to show the blinking spots. (**b-f**) Real-time blinking and laser activation traces for the samples in (a). Blinking events are separated into different panels, for each detected blinking event, XY (top) and time traces (bottom) are shown. XY traces are colour-coded by time (from black to orange) and overlaid with include- (green, dotted circle) and exclude- (red, dotted circle) ROIs; time traces show detected photon count per single-molecule localisation (orange), overlaid with laser illumination (magenta) and monitor

events (dashed line). All scale bars, 20 nm. See also Supplementary Methods 2.5 and Notes 3.2 for more details, and Supplementary Notes 3.4 for discussion regarding statistics and reproducibility.

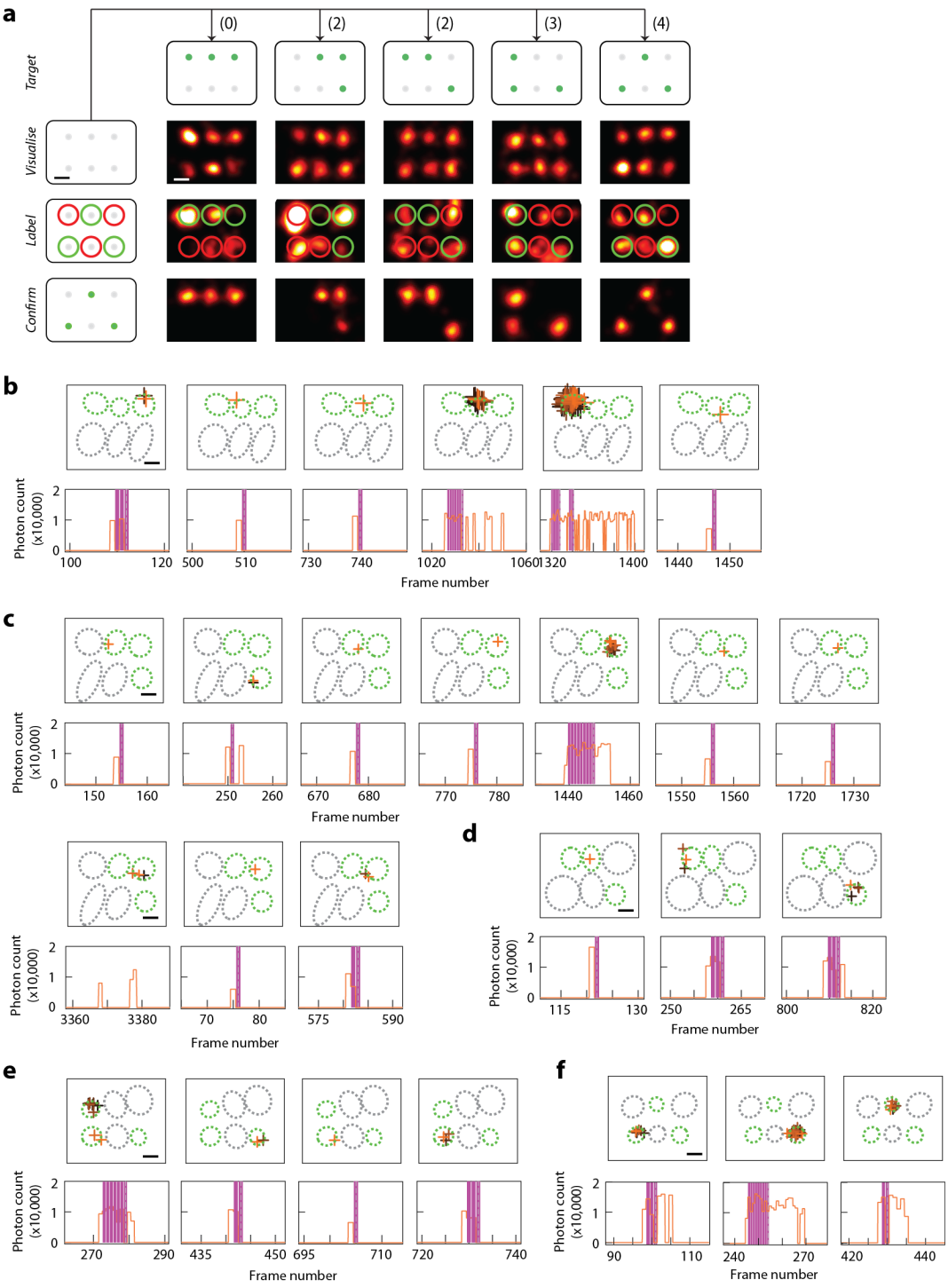

Supplementary Fig. 10 Representative examples of successful 3-point Action-PAINT single-molecule labelling.

(**a**) Schematics and super-resolution images of representative examples of successful labelling trials, at each stage of the experiment. Left column, schematics, right columns, super-resolution images. Top row, target labelling pattern ("target"), second row, pre-acquisition images ("visualise", image with asterisk was taken without candidate targets), third row, real-time labelling session images ("label"), bottom row,

post-acquisition images (“confirm”). In schematics, grey circles with a cross in schematics indicate markers, grey and green solid dots indicate markers, candidate (unlabelled) and successfully labelled target sites, respectively. Green and grey circles overlaid on both schematics and super-resolution images indicate desired and undesired target sites, respectively. Super-resolution images of real-time labelling session were normalised differently to show the blinking spots. (b-f) Real-time blinking and laser activation traces for the samples in (a). Blinking events are separated into different panels, for each detected blinking event, XY (top) and time traces (bottom) are shown. XY traces are colour-coded by time (from black to orange) and overlaid with include- (green, dotted circle) and exclude- (red, dotted circle) ROIs; time traces show detected photon count per single-molecule localisation (orange), overlaid with laser illumination (magenta) and monitor events (dashed line). All scale bars, 20 nm. See also Supplementary Methods 2.5 for more details, and Supplementary Notes 3.4 for discussion regarding statistics and reproducibility.

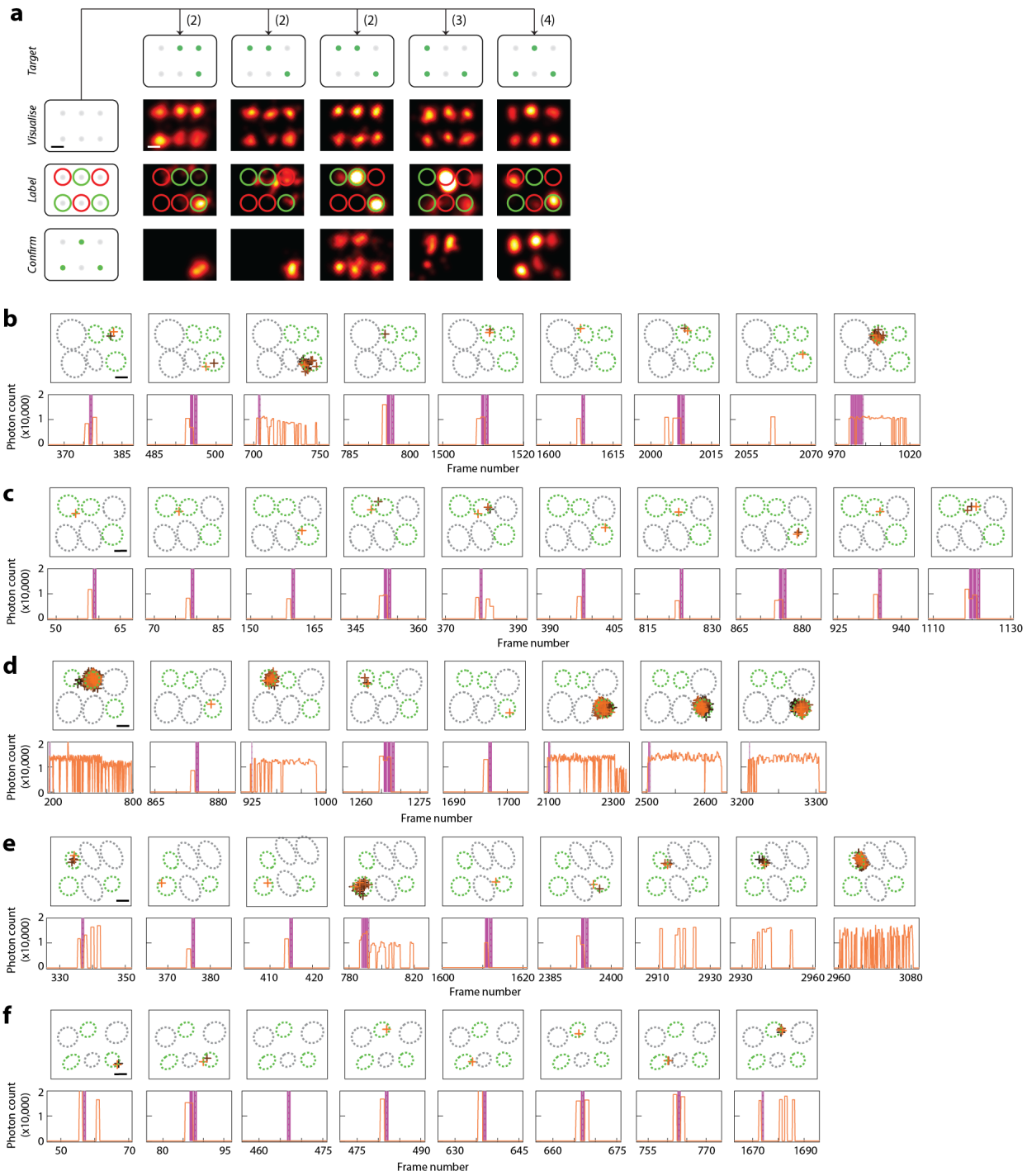

Supplementary Fig. 11 Representative examples of failed 3-point Action-PAINT single-molecule labelling.

(**a**) Schematics and super-resolution images of representative examples of successful labelling trials, at each stage of the experiment. Left column, schematics, right columns, super-resolution images. Top row, target labelling pattern ("target"), second row, pre-acquisition images ("visualise", image with asterisk was taken without candidate targets), third row, real-time labelling session images ("label"), bottom row, post-acquisition images ("confirm"). In schematics, grey circles with a cross in schematics indicate

markers, grey and green solid dots indicate markers, candidate (unlabelled) and successfully labelled target sites, respectively. Green and grey circles overlaid on both schematics and super-resolution images indicate desired and undesired target sites, respectively. Super-resolution images of real-time labelling session were normalised differently to show the blinking spots. (b-f) Real-time blinking and laser activation traces for the samples in (a). Blinking events are separated into different panels, for each detected blinking event, XY (top) and time traces (bottom) are shown. XY traces are colour-coded by time (from black to orange) and overlaid with include- (green, dotted circle) and exclude- (red, dotted circle) ROIs; time traces show detected photon count per single-molecule localisation (orange), overlaid with laser illumination (magenta) and monitor events (dashed line). All scale bars, 20 nm. See also Supplementary Methods 2.5 and Notes 3.2 for more details, and Supplementary Notes 3.4 for discussion regarding statistics and reproducibility.

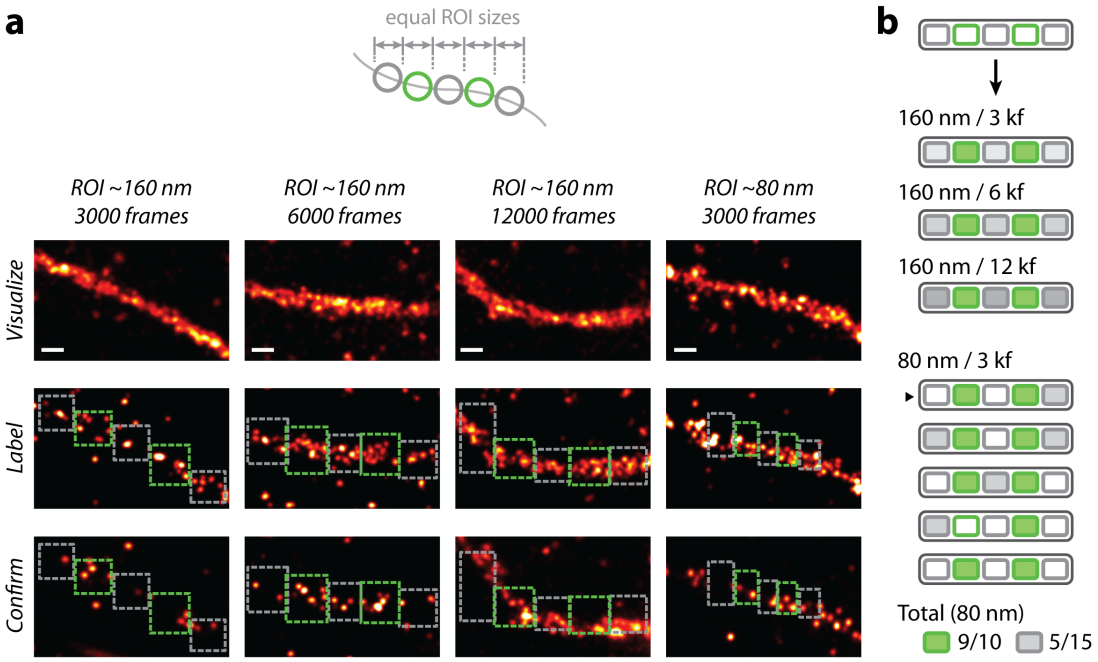

Supplementary Fig. 12 Representative examples of spatial patterning tests under different conditions on fixed microtubule samples.
(**a**) Examples of 2-target patterning on microtubules for different ROI-size and labelling session length. Top, schematics of desired labelling patterns and description for each condition, first row, pre-acquisition images, second row, real-time labelling session images, bottom row, post-acquisition images. (**b**) Schematic list of the experimental outcome for the four conditions tested. For 160 nm conditions, only one schematic is shown for each condition; for 80 nm tests, one schematic is shown for each experimental trial conducted. Successfully labelled targets are shaded green, undesired labels in exclude areas are shaded different grey levels to reflect different degree of off-target labelling. Arrow indicate the experiment shown in (a), last column. In all panels, green and grey circles in schematics indicate desired and undesired targets; green and grey dashed rectangles indicate experimental include- and exclude-ROIs, respectively. Scale bars in (a), 100 nm.

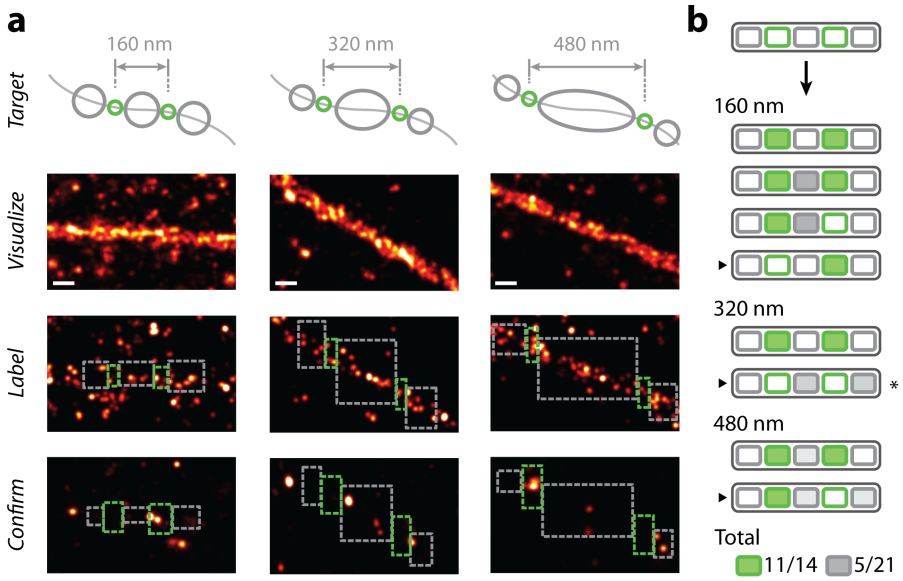

Supplementary Fig. 13 Representative examples of unsuccessful spatial patterning on fixed microtubule samples.
(**a**) Examples of unsuccessful 2-target patterning on microtubules for different inter-target spacing. Top row, schematics of desired labelling patterns, second row, pre-acquisition images, third row, real-time labelling session images, bottom row, post-acquisition images. (**b**) Schematic list of the outcome of 9 experimental trials. Successfully labelled targets are shaded green, undesired labels in exclude areas are shaded different grey levels to reflect the difference in exclude area. Arrows indicate experiments shown in (a). (*) indicate experiment excluded from statistics, due to likely sample movement between labelling and post-acquisition sessions. In all panels, green and grey circles in schematics indicate desired and undesired targets; green and grey dashed rectangles indicate experimental include- and exclude-ROIs, respectively. ROIs in last row (post-acquisition images) are adjusted by 20 nm edge buffer, according to the overall localisation and labelling precision. Scale bars in (a), 100 nm. See Supplementary Methods and Notes 3.3 for more details regarding crosslinking efficiency and specificity calculation, and edge-buffered ROIs, and Supplementary Notes 3.4 for discussion regarding statistics and reproducibility.

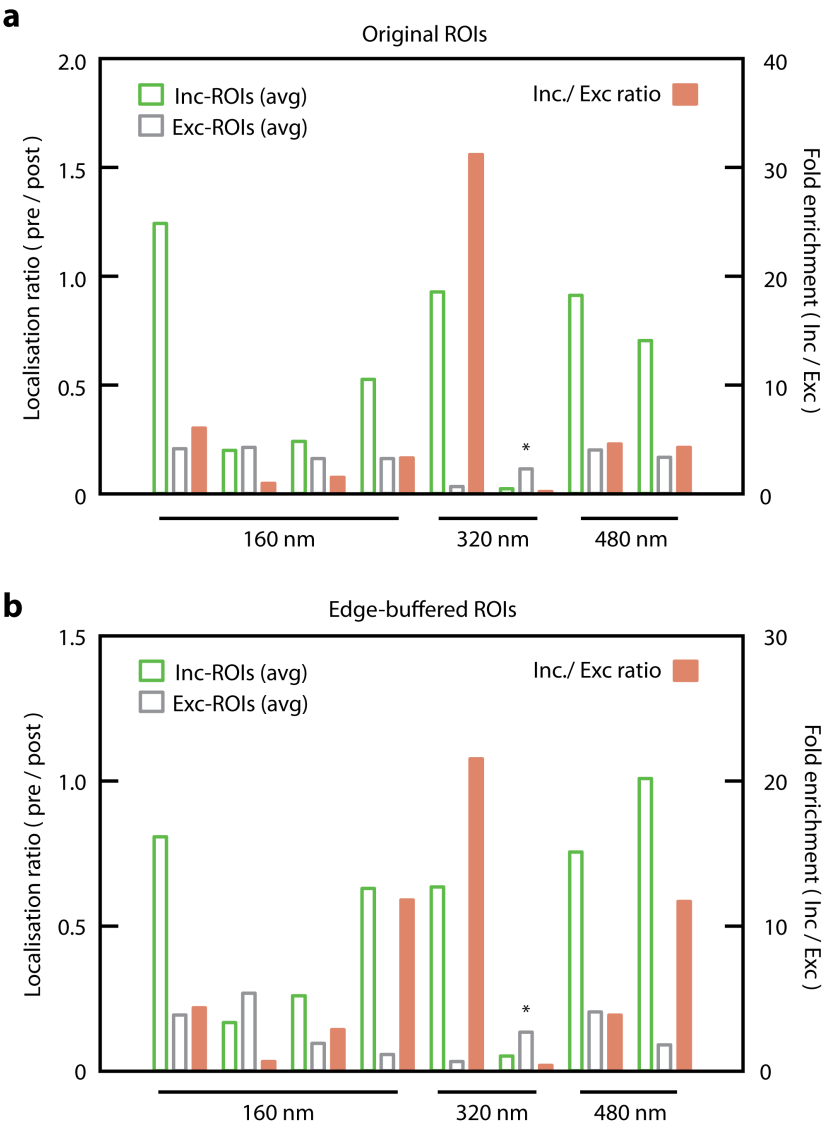

Supplementary Fig. 14 Crosslinking efficiency and specificity assayed for 2-point microtubule labelling with varying inter-target spacing

(**a-b**) Comparison of crosslinking efficiency and specificity assayed with original (a) and edge-buffered (b) ROIs. In each panel, green and grey coloured hollow bars indicate crosslinking efficiency (i.e. localisation ratio between pre- and post-acquisition images, left axis), orange filled bars indicate crosslinking specificity (i.e. fold enrichment between include- and exclude-ROIs, right axis). (*) indicate experiment excluded from statistics, due to likely sample movement between labelling and post-acquisition sessions. See Supplementary Methods and Notes 3.3 for more details regarding crosslinking efficiency and specificity calculation, and edge-buffered ROIs.

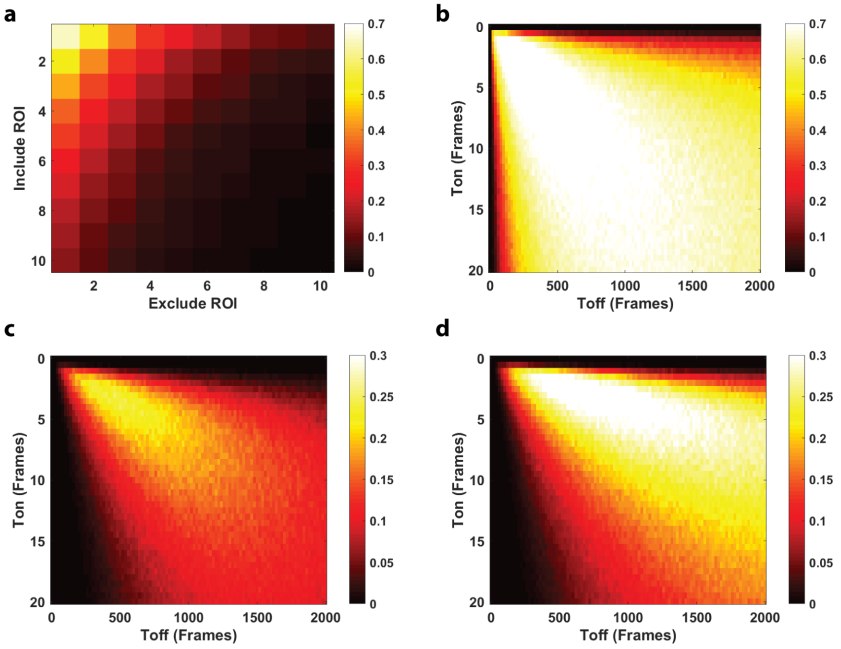

Supplementary Fig. 15 Simulation for Action-PAINT experiments
(**a**) Overall Action-PAINT labelling success rate as a function of different number of include- and exclude-ROIs, with typical binding on-time and off-time, and total imaging length set to 5000 frames. (**b**) Overall Action-PAINT labelling success rate of 2-choose-1 labelling experiment as a function of characteristic binding on-time and off-time, with total imaging length set to 5000 frames. (**c**) Overall Action-PAINT labelling success rate of 6-choose-3 labelling experiment as a function of characteristic binding on-time and off-time, with total imaging length set to 5000 frames. (**d**) Overall Action-PAINT labelling success rate of 6-choose-3 labelling experiment as a function of characteristic binding on-time and off-time, with total imaging length set to 10000 frames. See Supplementary Methods 2.10 for more details regarding the simulations.

2. Tables

Supplementary Table 1 | List of staple sequences for self-assembly of the rectangular DNA origami nanostructure

All staple strands for self-assembly of the rectangular DNA origami nanostructure, used as a template for assembly of various imaging standard samples. The colours of staples match those in Fig. S3. Grey: unmodified staple strands. Light orange and crimson: strands with biotin extension for surface fixation, and strands with modified wiring pattern to accommodate those orange ones.

Strand ID	Sequence	Colour	Notes
0[47]1[31]	AGAAAGGAACAACTAAAGGAATTCAAAAAAA		Structure staples
0[79]1[63]	ACAACTTTCAACAGTTTCAGCGGATGTATCGG		Structure staples
0[111]1[95]	TAAATGAATTTTCTGTATGGGATTAATTTCTT		Structure staples
0[143]1[127]	TCTAAAGTTTTGTCGTCTTTCCAGCCGACAA		Structure staples
0[175]0[144]	TCCACAGACAGCCCTCATAGTTAGCGTAACGA		Structure staples
0[207]1[191]	TCACCAGTACAAACTACAACGCCTAGTACCAG		Structure staples
0[239]1[223]	AGGAACCCATGTACCGTAACACTTGATATAA		Structure staples
0[271]1[255]	CCACCCTCATTTTCAGGGATAGCAACCGTACT		Structure staples
1[32]3[31]	AGGCTCCAGAGGCTTTGAGGACACGGGTAA		Structure staples
1[96]3[95]	AAACAGCTTTTTGCGGGATCGTCAACACTAAA		Structure staples
1[160]2[144]	TTAGGATTGGCTGAGACTCCTCAATAACCGAT		Structure staples
1[224]3[223]	GTATAGCAAACAGTTAATGCCCAATCCTCA		Structure staples
2[47]0[48]	ACGGCTACAAAAGGAGCCTTTAATGTGAGAAT		Structure staples
2[79]0[80]	CAGCGAAACTTGCTTTCGAGGTGTTGCTAA		Structure staples
2[111]0[112]	AAGGCCGCTGATACCGATAGTTGCGACGTTAG		Structure staples
2[143]1[159]	ATATTCGGAACCATCGCCCACGCAGAGAAGGA		Structure staples
2[175]0[176]	TATTAAGAAGCGGGGTTTTGCTCGTAGCAT		Structure staples
2[207]0[208]	TTTCGGAAGTGCCGTCGAGAGGGTGAGTTTCG		Structure staples
2[239]0[240]	GCCCGTATCCGGAATAGGTGTATCAGCCCAAT		Structure staples
2[271]0[272]	GTTTTAACTTAGTACCGCCACCCAGAGCCA		Structure staples
3[32]5[31]	AATACGTTTGAAAGAGGACAGACTGACCTT		Structure staples
3[96]5[95]	ACACTCATCCATGTTACTTAGCCGAAAGCTGC		Structure staples
3[160]4[144]	TTGACAGGCCACCACCAGAGCCGCGATTTGTA		Structure staples
3[224]5[223]	TTAAAGCCAGAGCCGCCACCCTCGACAGAA		Structure staples
4[47]2[48]	GACCAACTAATGCCACTACGAAGGGGGTAGCA		Structure staples
4[79]2[80]	GCGCAGACAAGAGGCAAAAGAATCCCTCAG		Structure staples
4[111]2[112]	GACCTGCTCTTTGACCCCCAGCGAGGGAGTTA		Structure staples

4[143]3[159]	TCATCGCCAACAAAGTACAACGGACGCCAGCA		Structure staples
4[175]2[176]	CACCAGAAAGGTTGAGGCAGGTCATGAAAG		Structure staples
4[207]2[208]	CCACCCTCTATTCACAAACAAATACCTGCCTA		Structure staples
4[239]2[240]	GCCTCCCTCAGAATGGAAAGCGCAGTAACAGT		Structure staples
4[271]2[272]	AAATCACCTTCCAGTAAGCGTCAGTAATAA		Structure staples
5[32]7[31]	CATCAAGTAAAACGAACTAACGAGTTGAGA		Structure staples
5[96]7[95]	TCATTCAGATGCGATTTTAAGAACAGGCATAG		Structure staples
5[160]6[144]	GCAAGGCCTCACCAGTAGCACCATGGGCTTGA		Structure staples
5[224]7[223]	TCAAGTTTCATTAAAGGTGAATATAAAAGA		Structure staples
6[47]4[48]	TACGTTAAAGTAATCTTGACAAGAACCGAACT		Structure staples
6[79]4[80]	TTATACCACCAAATCAACGTAACGAACGAG		Structure staples
6[111]4[112]	ATTACCTTTGAATAAGGCTTGCCCAAATCCGC		Structure staples
6[143]5[159]	GATGGTTTGAACGAGTAGTAAATTTACCATTA		Structure staples
6[175]4[176]	CAGCAAAAGGAAACGTCACCAATGAGCCGC		Structure staples
6[207]4[208]	TCACCGACGCACCGTAATCAGTAGCAGAACCG		Structure staples
6[239]4[240]	GAAATTATTGCCTTTAGCGTCAGACCGGAACC		Structure staples
6[271]4[272]	ACCGATTGTCGGCATTTTCGGTCATAATCA		Structure staples
7[32]9[31]	TTTAGGACAAATGCTTTAAACAATCAGGTC		Structure staples
7[56]9[63]	ATGCAGATACATAACGGGAATCGTCATAAATAAAGCAAAG		Structure staples
7[96]9[95]	TAAGAGCAAATGTTTAGACTGGATAGGAAGCC		Structure staples
7[120]9[127]	CGTTTACCAGACGACAAAGAAGTTTTGCCATAATTCGA		Structure staples
7[160]8[144]	TTATTACGAAGAACTGGCATGATTGCGAGAGG		Structure staples
7[184]9[191]	CGTAGAAAATACATACCGAGGAAACGCAATAAGAAGCGCA		Structure staples
7[224]9[223]	AACGCAAAGATAGCCGAACAAACCCTGAAC		Structure staples
7[248]9[255]	GTTTATTTTGTCACAATCTTACCGAAGCCCTTTAATATCA		Structure staples
8[47]6[48]	ATCCCCCTATACCACATTCAACTAGAAAAATC		Structure staples
8[79]6[80]	AATACTGCCCAAAAGGAATTACGTGGCTCA		Structure staples
8[111]6[112]	AATAGTAAACACTATCATAACCCTCATTGTGA		Structure staples
8[143]7[159]	CTTTTGCAGATAAAAACCAAAATAAAGACTCC		Structure staples
8[175]6[176]	ATACCCAACAGTATGTTAGCAAATTAGAGC		Structure staples
8[207]6[208]	AAGGAAACATAAAGGTGGCAACATTATCACCG		Structure staples
8[239]6[240]	AAGTAAGCAGACACCACGGAATAATATTGACG		Structure staples
8[271]6[272]	AATAGCTATCAATAGAAAATTCAACATTCA		Structure staples
9[32]11[31]	TTTACCCCAACATGTTTTAAATTTCCATAT		Structure staples
9[64]11[63]	CGGATTGCAGAGCTTAATTGCTGAAACGAGTA		Structure staples
9[96]11[95]	CGAAAGACTTTGATAAGAGGTCATATTTCGCA		Structure staples
9[128]11[127]	GCTTCAATCAGGATTAGAGAGTTATTTTCA		Structure staples
9[160]10[144]	AGAGAGAAAAAAATGAAAATAGCAAGCAAACT		Structure staples

9[192]11[191]	TTAGACGGCCAAATAAGAAACGATAGAAGGCT		Structure staples
9[224]11[223]	AAAGTCACAAAATAAACAGCCAGCGTTTTA		Structure staples
9[256]11[255]	GAGAGATAGAGCGTCTTTCCAGAGGTTTTGAA		Structure staples
10[47]8[48]	CTGTAGCTTGACTATTATAGTCAGTTCATTGA		Structure staples
10[79]8[80]	GATGGCTTATCAAAAAGATTAAGAGCGTCC		Structure staples
10[111]8[112]	TTGCTCCTTTCAAATATCGCGTTTGAGGGGGT		Structure staples
10[143]9[159]	CCAACAGGAGCGAACCAGACCGGAGCCTTTAC		Structure staples
10[175]8[176]	TTAACGTCTAACATAAAAACAGGTAACGGA		Structure staples
10[207]8[208]	ATCCCAATGAGAATTAACTGAACAGTTACCAG		Structure staples
10[239]8[240]	GCCAGTTAGAGGGTAATTGAGCGCTTTAAGAA		Structure staples
10[271]8[272]	ACGCTAACACCCACAAGAATTGAAAATAGC		Structure staples
11[32]13[31]	AACAGTTTTGTACCAAAAACATTTTATTTC		Structure staples
11[64]13[63]	GATTTAGTCAATAAAGCCTCAGAGAACCCTCA		Structure staples
11[96]13[95]	AATGGTCAACAGGCAAGGCAAAGAGTAATGTG		Structure staples
11[128]13[127]	TTTGGGGATAGTAGTAGCATTAAAAGGCCG		Structure staples
11[160]12[144]	CCAATAGCTCATCGTAGGAATCATGGCATCAA		Structure staples
11[192]13[191]	TATCCGGTCTCATCGAGAACAAGCGACAAAAG		Structure staples
11[224]13[223]	GCGAACCTCCAAGAACGGGTATGACAATAA		Structure staples
11[256]13[255]	GCCTTAAACCAATCAATAATCGGCACGCGCCT		Structure staples
12[47]10[48]	TAAATCGGGATTCCCAATTCTGCGATATAATG		Structure staples
12[79]10[80]	AAATTAAGTTGACCATTAGATACTTTTGCG		Structure staples
12[111]10[112]	TAAATCATATAACCTGTTTAGCTAACCTTTAA		Structure staples
12[143]11[159]	TTCTACTACGCGAGCTGAAAAGGTTACCGCGC		Structure staples
12[175]10[176]	TTTTATTTAAGCAAATCAGATATTTTTTGT		Structure staples
12[207]10[208]	GTACCGCAATTCTAAGAACGCGAGTATTATTT		Structure staples
12[239]10[240]	CTTATCATTCCCGACTTGCGGGAGCCTAATTT		Structure staples
12[271]10[272]	TGTAGAAATCAAGATTAGTTGCTCTTACCA		Structure staples
13[32]15[31]	AACGCAAAATCGATGAACGGTACCGGTTGA		Structure staples
13[64]15[63]	TATATTTTGTCATTGCCTGAGAGTGGAAGATT		Structure staples
13[96]15[95]	TAGGTAAACTATTTTTGAGAGATCAAACGTTA		Structure staples
13[128]15[127]	GAGACAGCTAGCTGATAAATTAATTTTTGT		Structure staples
13[160]14[144]	GTAATAAGTTAGGCAGAGGCATTTATGATATT		Structure staples
13[192]15[191]	GTAAAGTAATCGCCATATTTAACAAAACTTTT		Structure staples
13[224]15[223]	ACAACATGCCAACGCTCAACAGTCTTCTGA		Structure staples
13[256]15[255]	GTTTATCAATATGCGTTATACAAACCGACCGT		Structure staples
14[47]12[48]	AACAAGAGGGATAAAAATTTTTAGCATAAAGC		Structure staples
14[79]12[80]	GCTATCAGAAATGCAATGCCTGAATTAGCA		Structure staples
14[111]12[112]	GAGGGTAGGATTCAAAAGGGTGAGACATCCAA		Structure staples

14[143]13[159]	CAACCGTTTCAAATCACCATCAATTCGAGCCA		Structure staples
14[175]12[176]	CATGTAATAGAATATAAAGTACCAAGCCGT		Structure staples
14[207]12[208]	AATTGAGAATTCTGTCCAGACGACTAAACCAA		Structure staples
14[239]12[240]	AGTATAAAGTTCAGCTAATGCAGATGTCTTTC		Structure staples
14[271]12[272]	TTAGTATCACAATAGATAAGTCCACGAGCA		Structure staples
15[32]17[31]	TAATCAGCGGATTGACCGTAATCGTAACCG		Structure staples
15[96]17[95]	ATATTTTGGCTTTCATCAACATTATCCAGCCA		Structure staples
15[160]16[144]	ATCGCAAGTATGTAAATGCTGATGATAGGAAC		Structure staples
15[224]17[223]	CCTAAATCAAAATCATAGGTCTAAACAGTA		Structure staples
16[47]14[48]	ACAAACGGAAAAGCCCCAAAAACACTGGAGCA		Structure staples
16[79]14[80]	GCGAGTAAAAATATTTAAATTGTTACAAAG		Structure staples
16[111]14[112]	TGTAGCCATTAAAATTCGCATTAAATGCCGGA		Structure staples
16[143]15[159]	GCCATCAAGCTCATTTTTTAACCACAAATCCA		Structure staples
16[175]14[176]	TATAACTAACAAAGAACGCGAGAACGCCAA		Structure staples
16[207]14[208]	ACCTTTTTATTTTAGTTAATTTCATAGGGCTT		Structure staples
16[239]14[240]	GAATTTATTTAATGGTTTGAAATATTCTTACC		Structure staples
16[271]14[272]	CTTAGATTTAAGGCGTTAAATAAAGCCTGT		Structure staples
17[32]19[31]	TGCATCTTTCCCAGTCACGACGGCCTGCAG		Structure staples
17[96]19[95]	GCTTTCCGATTACGCCAGCTGGCGGCTGTTTC		Structure staples
17[160]18[144]	AGAAAACAAAGAAGATGATGAAACAGGCTGCG		Structure staples
17[224]19[223]	CATAAATCTTTGAATACCAAGTGTTAGAAC		Structure staples
18[47]16[48]	CCAGGGTTGCCAGTTTGAGGGGACCCGTGGGA		Structure staples
18[79]16[80]	GATGTGCTTCAGGAAGATCGCACAATGTGA		Structure staples
18[111]16[112]	TCTTCGCTGCACCGCTTCTGGTGCGGCCTTCC		Structure staples
18[143]17[159]	CAACTGTTGCGCCATTCGCCATTCAAACATCA		Structure staples
18[175]16[176]	CTGAGCAAAAATTAATTACATTTTGGGTTA		Structure staples
18[207]16[208]	CGCGCAGATTACCTTTTTTAATGGGAGAGACT		Structure staples
18[239]16[240]	CCTGATTGCAATATATGTGAGTGATCAATAGT		Structure staples
18[271]16[272]	CTTTTACAAAATCGTCGCTATTAGCGATAG		Structure staples
19[32]21[31]	GTCGACTTCGGCCAACGCGCGGGGTTTTTC		Structure staples
19[96]21[95]	CTGTGTGATTGCGTTGCGCTCACTAGAGTTGC		Structure staples
19[160]20[144]	GCAATTCACATATTCCTGATTATCAAAGTGTA		Structure staples
19[224]21[223]	CTACCATAGTTTGAGTAACATTTAAAATAT		Structure staples
20[47]18[48]	TTAATGAACTAGAGGATCCCCGGGGGGTAACG		Structure staples
20[79]18[80]	TTCCAGTCGTAATCATGGTCATAAAAGGGG		Structure staples
20[111]18[112]	CACATTAAAATTGTTATCCGCTCATGCGGGCC		Structure staples
20[143]19[159]	AAGCCTGGTACGAGCCGGAAGCATAGATGATG		Structure staples
20[175]18[176]	ATTATCATTCAATATAATCCTGACAATTAC		Structure staples

20[207]18[208]	GCGGAACATCTGAATAATGGAAGGTACAAAAT		Structure staples
20[239]18[240]	ATTTTAAAATCAAAATTATTTGCACGGATTCG		Structure staples
20[271]18[272]	CTCGTATTAGAAATTGCGTAGATACAGTAC		Structure staples
21[32]23[31]	TTTTCACTCAAAGGGCGAAAAACCATCACC		Structure staples
21[56]23[63]	AGCTGATTGCCCTTCAGAGTCCACTATTAAAGGGTGCCGT		Structure staples
21[96]23[95]	AGCAAGCGTAGGGTTGAGTGTTGTAGGGAGCC		Structure staples
21[120]23[127]	CCCAGCAGGCGAAAAATCCCTTATAAATCAAGCCGGCG		Structure staples
21[160]22[144]	TCAATATCGAACCTCAAATATCAATTCCGAAA		Structure staples
21[184]23[191]	TCAACAGTTGAAAGGAGCAAATGAAAAATCTAGAGATAGA		Structure staples
21[224]23[223]	CTTTAGGGCCTGCAACAGTGCCAATACGTG		Structure staples
21[248]23[255]	AGATTAGAGCCGTCAAAAAACAGAGGTGAGGCCTATTAGT		Structure staples
22[47]20[48]	CTCCAACGCAGTGAGACGGGCAACCAGCTGCA		Structure staples
22[79]20[80]	TGGAACAACCGCCTGGCCCTGAGGCCCGCT		Structure staples
22[111]20[112]	GCCCGAGAGTCCACGCTGGTTTGCAGCTAACT		Structure staples
22[143]21[159]	TCGGCAAATCCTGTTTGATGGTGGACCCTCAA		Structure staples
22[175]20[176]	ACCTTGCTTGGTCAGTTGGCAAAGAGCGGA		Structure staples
22[207]20[208]	AGCCAGCAATTGAGGAAGGTTATCATCATTTT		Structure staples
22[239]20[240]	TTAACACCAGCACTAACAACTAATCGTTATTA		Structure staples
22[271]20[272]	CAGAAGATTAGATAATACATTTGTCGACAA		Structure staples
23[32]22[48]	CAAATCAAGTTTTTTGGGGTCGAAACGTGGA		Structure staples
23[64]22[80]	AAAGCACTAAATCGGAACCCTAATCCAGTT		Structure staples
23[96]22[112]	CCCGATTTAGAGCTTGACGGGGAAAAAGAATA		Structure staples
23[128]23[159]	AACGTGGCGAGAAAGGAAGGGAAACCAGTAA		Structure staples
23[160]22[176]	TAAAAGGGACATTCTGGCCAACAAAGCATC		Structure staples
23[192]22[208]	ACCCTTCTGACCTGAAAGCGTAAGACGCTGAG		Structure staples
23[224]22[240]	GCACAGACAATATTTTTGAATGGGGTCAGTA		Structure staples
23[256]22[272]	CTTTAATGCGCGAACTGATAGCCCCACCAG		Structure staples
1[64]4[64]	TTTATCAGGACAGCATCGGAACGACACCAACCTAAAACGAGGTCAATC		Biotin helper strand
1[128]4[128]	TGACAACTCGCTGAGGCTTGCATTATACCAAGCGCGATGATAAA		Biotin helper strand
1[192]4[192]	GCGGATAACCTATTATTCTGAAACAGACGATTGGCCTTGAAGAGCCAC		Biotin helper strand
1[256]4[256]	CAGGAGGTGGGGTCAGTGCCTTGAGTCTCTGAATTTACCGGGAACCAG		Biotin helper strand
15[64]18[64]	GTATAAGCCAACCCGTCGGATTCTGACGACAGTATCGGCCGCAAGGCG		Biotin helper strand
15[128]18[128]	TAAATCAAAATAATTCGCGTCTCGGAAACCAGGCAAAGGGAAGG		Biotin helper strand
15[192]18[192]	TCAAATATAACCTCCGGCTTAGGTAACAATTTCATTTGAAGGCGAATT		Biotin helper strand
15[256]18[256]	GTGATAAAAAGACGCTGAGAAGAGATAACCTTGCTTCTGTTCGGGAGA		Biotin helper strand
4[63]6[56]	Biotin-TTTTATAAGGGAACCGGATATTCATTACGTCAGGACGTTGGGAA		Biotin-labelled strand
4[127]6[120]	Biotin-TTTTTTGTGTCGTGACGAGAAACACCAAATTTCAACTTTAAT		Biotin-labelled strand
4[191]6[184]	Biotin-TTTTCACCCTCAGAAACCATCGATAGCATTGAGCCATTTGGGAA		Biotin-labelled strand

4[255]6[248]	Biotin-TTTTAGCCACCACTGTAGCGCGTTTTCAAGGGAGGGAAGGTAAA		Biotin-labelled strand
18[63]20[56]	Biotin-TTTTATTAAGTTTACCGAGCTCGAATTCGGGAAACCTGTCGTGC		Biotin-labelled strand
18[127]20[120]	Biotin-TTTTGCGATCGGCAATTCCACACAACAGGTGCCTAATGAGTG		Biotin-labelled strand
18[191]20[184]	Biotin-TTTTATTCATTTTTGTTTGGATTATACTAAGAAACCACCAGAAG		Biotin-labelled strand
18[255]20[248]	Biotin-TTTTAACAATAACGTAAAACAGAAATAAAAATCCTTTGCCCGAA		Biotin-labelled strand

Supplementary Table 2 | List of DNA-PAINT extension sequences for Action-PAINT labelling targets, position marker and drift marker

Table 2a | Sequences for Action-PAINT candidate labelling targets, for use with AGv3 sequence

Strand ID	Replace this sequence	With this sequence	Notes
4[239]2[240]	GCCTCCCTCAGAATGGAAAGCGCAGTAACAGT	GCCTCCCTCAGAATGGAAAGCGCAGTAACAGTTTATGCTTCGA	1-point target
20[47]18[48]	TTAATGAACTAGAGGATCCCCGGGGGGTAACG	TTAATGAACTAGAGGATCCCCGGGGGGTAACGTTATGCTTCGA	1-point target
4[47]2[48]	GACCAACTAATGCCACTACGAAGGGGGTAGCA	GACCAACTAATGCCACTACGAAGGGGGTAGCATTATGCTTCGA	3-point target
4[143]3[159]	TCATCGCCAACAAAGTACAACGGACGCCAGCA	TCATCGCCAACAAAGTACAACGGACGCCAGCATTATGCTTCGA	3-point target
4[239]2[240]	GCCTCCCTCAGAATGGAAAGCGCAGTAACAGT	GCCTCCCTCAGAATGGAAAGCGCAGTAACAGTTTATGCTTCGA	3-point target
20[47]18[48]	TTAATGAACTAGAGGATCCCCGGGGGGTAACG	TTAATGAACTAGAGGATCCCCGGGGGGTAACGTTATGCTTCGA	3-point target
20[143]19[159]	AAGCCTGGTACGAGCCGGAAGCATAGATGATG	AAGCCTGGTACGAGCCGGAAGCATAGATGATGTTATGCTTCGA	3-point target
20[239]18[240]	ATTTTAAAATCAAAATTATTTGCACGGATTCG	ATTTTAAAATCAAAATTATTTGCACGGATTCGTTATGCTTCGA	3-point target

Table 2b | Sequences for Action-PAINT candidate labelling targets, for use with E1v3 sequence

Strand ID	Replace this sequence	With this sequence	Notes
4[239]2[240]	GCCTCCCTCAGAATGGAAAGCGCAGTAACAGT	GCCTCCCTCAGAATGGAAAGCGCAGTAACAGTTTATGATTCGAT	1-point target
20[47]18[48]	TTAATGAACTAGAGGATCCCCGGGGGGTAACG	TTAATGAACTAGAGGATCCCCGGGGGGTAACGTTATGATTCGAT	1-point target
4[47]2[48]	GACCAACTAATGCCACTACGAAGGGGGTAGCA	GACCAACTAATGCCACTACGAAGGGGGTAGCATTATGATTCGAT	3-point target
4[143]3[159]	TCATCGCCAACAAAGTACAACGGACGCCAGCA	TCATCGCCAACAAAGTACAACGGACGCCAGCATTATGATTCGAT	3-point target
4[239]2[240]	GCCTCCCTCAGAATGGAAAGCGCAGTAACAGT	GCCTCCCTCAGAATGGAAAGCGCAGTAACAGTTTATGATTCGAT	3-point target
20[47]18[48]	TTAATGAACTAGAGGATCCCCGGGGGGTAACG	TTAATGAACTAGAGGATCCCCGGGGGGTAACGTTATGATTCGAT	3-point target
20[143]19[159]	AAGCCTGGTACGAGCCGGAAGCATAGATGATG	AAGCCTGGTACGAGCCGGAAGCATAGATGATGTTATGATTCGAT	3-point target
20[239]18[240]	ATTTTAAAATCAAAATTATTTGCACGGATTCG	ATTTTAAAATCAAAATTATTTGCACGGATTCGTTATGATTCGAT	3-point target

Table 2c | Sequences for Action-PAINT position markers for 1-point labelling experiments

Strand ID	Replace this sequence	With this sequence	Notes
4[175]2[176]	CACCAGAAAGGTTGAGGCAGGTCATGAAAG	CACCAGAAAGGTTGAGGCAGGTCATGAAAGTTATACATCTA	1-point marker
12[239]10[240]	CTTATCATTCCCGACTTGCGGGAGCCTAATTT	CTTATCATTCCCGACTTGCGGGAGCCTAATTTTTATACATCTA	1-point marker

12[47]10[48]	TAAATCGGGATTCCCAATTCTGCGATATAATG	TAAATCGGGATTCCCAATTCTGCGATATAATGTTATACATCTA	1-point marker
20[111]18[112]	CACATTAAAATTGTTATCCGCTCATGCGGGCC	CACATTAAAATTGTTATCCGCTCATGCGGGCCTTATACATCTA	1-point marker

Table 2d | Sequences for 20 nm grid used as drift correction marker

Strand ID	Replace this sequence	With this sequence	Notes
4[239]2[240]	GCCTCCCTCAGAATGGAAAGCGCAGTAACAGT	GCCTCCCTCAGAATGGAAAGCGCAGTAACAGTTTATGAATCTA	20-nm-grid
4[175]2[176]	CACCAGAAAGGTTGAGGCAGGTCATGAAAG	CACCAGAAAGGTTGAGGCAGGTCATGAAAGTTATGAATCTA	20-nm-grid
4[111]2[112]	GACCTGCTCTTTGACCCCCAGCGAGGGAGTTA	GACCTGCTCTTTGACCCCCAGCGAGGGAGTTATTATGAATCTA	20-nm-grid
4[47]2[48]	GACCAACTAATGCCACTACGAAGGGGGTAGCA	GACCAACTAATGCCACTACGAAGGGGGTAGCATTATGAATCTA	20-nm-grid
12[239]10[240]	CTTATCATTCCCGACTTGCGGGAGCCTAATTT	CTTATCATTCCCGACTTGCGGGAGCCTAATTTTTATGAATCTA	20-nm-grid
12[175]10[176]	TTTTATTTAAGCAAATCAGATATTTTTTGT	TTTTATTTAAGCAAATCAGATATTTTTTGTTTATGAATCTA	20-nm-grid
12[111]10[112]	TAAATCATATAACCTGTTTAGCTAACCTTTAA	TAAATCATATAACCTGTTTAGCTAACCTTTAATTATGAATCTA	20-nm-grid
12[47]10[48]	TAAATCGGGATTCCCAATTCTGCGATATAATG	TAAATCGGGATTCCCAATTCTGCGATATAATGTTATGAATCTA	20-nm-grid
20[239]18[240]	ATTTTAAAATCAAAATTATTTGCACGGATTCG	ATTTTAAAATCAAAATTATTTGCACGGATTCGTTATGAATCTA	20-nm-grid
20[175]18[176]	ATTATCATTCAATATAATCCTGACAATTAC	ATTATCATTCAATATAATCCTGACAATTACTTATGAATCTA	20-nm-grid
20[111]18[112]	CACATTAAAATTGTTATCCGCTCATGCGGGCC	CACATTAAAATTGTTATCCGCTCATGCGGGCCTTATGAATCTA	20-nm-grid
20[47]18[48]	TTAATGAACTAGAGGATCCCCGGGGGGTAACG	TTAATGAACTAGAGGATCCCCGGGGGGTAACGTTATGAATCTA	20-nm-grid

Supplementary Table 3 ▏Sequence for M13mp18 phage single-stranded DNA scaffold

TTCCCTTCCTTTCTCGCCACGTTCGCCGGCTTTCCCCGTCAAGCTCTAAATCGGGGGCTCCCTTTAGGGTTCCGATTTAGTGCTTTACGGCACCTCGACCCCAAAAAACT
TGATTTGGGTGATGGTTCACGTAGTGGGCCATCGCCCTGATAGACGGTTTTTCGCCCTTTGACGTTGGAGTCCACGTTCTTTAATAGTGGACTCTTGTTCCAAACTGGAA
CAACACTCAACCCTATCTCGGGCTATTCTTTTGATTTATAAGGGATTTTGCCGATTTCGGAACCACCATCAAACAGGATTTTCGCCTGCTGGGGCAAACCAGCGTGGACC
GCTTGCTGCAACTCTCTCAGGGCCAGGCGGTGAAGGGCAATCAGCTGTTGCCCGTCTCACTGGTGAAAAGAAAAACCACCCTGGCGCCCAATACGCAAACCGCCTCTCCC
CGCGCGTTGGCCGATTCATTAATGCAGCTGGCACGACAGGTTTCCCGACTGGAAAGCGGGCAGTGAGCGCAACGCAATTAATGTGAGTTAGCTCACTCATTAGGCACCCC
AGGCTTTACACTTTATGCTTCCGGCTCGTATGTTGTGTGGAATTGTGAGCGGATAACAATTTCACACAGGAAACAGCTATGACCATGATTACGAATTCGAGCTCGGTACC
CGGGGATCCTCTAGAGTCGACCTGCAGGCATGCAAGCTTGGCACTGGCCGTCGTTTTACAACGTCGTGACTGGGAAAACCCTGGCGTTACCCAACTTAATCGCCTTGCAG
CACATCCCCCTTTCGCCAGCTGGCGTAATAGCGAAGAGGCCCGCACCGATCGCCCTTCCCAACAGTTGCGCAGCCTGAATGGCGAATGGCGCTTTGCCTGGTTTCCGGCA
CCAGAAGCGGTGCCGGAAAGCTGGCTGGAGTGCGATCTTCCTGAGGCCGATACTGTCGTCGTCCCCTCAAACTGGCAGATGCACGGTTACGATGCGCCCATCTACACCAA
CGTGACCTATCCCATTACGGTCAATCCGCCGTTTGTTCCCACGGAGAATCCGACGGGTTGTTACTCGCTCACATTTAATGTTGATGAAAGCTGGCTACAGGAAGGCCAGA
CGCGAATTATTTTTGATGGCGTTCCTATTGGTTAAAAAATGAGCTGATTTAACAAAAATTTAATGCGAATTTTAACAAAATATTAACGTTTACAATTTAAATATTTGCTT
ATACAATCTTCCTGTTTTTGGGGCTTTTCTGATTATCAACCGGGGTACATATGATTGACATGCTAGTTTTACGATTACCGTTCATCGATTCTCTTGTTTGCTCCAGACTC
TCAGGCAATGACCTGATAGCCTTTGTAGATCTCTCAAAAATAGCTACCCTCTCCGGCATTAATTTATCAGCTAGAACGGTTGAATATCATATTGATGGTGATTTGACTGT
CTCCGGCCTTTCTCACCCTTTTGAATCTTTACCTACACATTACTCAGGCATTGCATTTAAAATATATGAGGGTTCTAAAAATTTTTATCCTTGCGTTGAAATAAAGGCTT
CTCCCGCAAAAGTATTACAGGGTCATAATGTTTTTGGTACAACCGATTTAGCTTTATGCTCTGAGGCTTTATTGCTTAATTTTGCTAATTCTTTGCCTTGCCTGTATGAT
TTATTGGATGTTAATGCTACTACTATTAGTAGAATTGATGCCACCTTTTCAGCTCGCGCCCCAAATGAAAATATAGCTAAACAGGTTATTGACCATTTGCGAAATGTATC
TAATGGTCAAACTAAATCTACTCGTTCGCAGAATTGGGAATCAACTGTTATATGGAATGAAACTTCCAGACACCGTACTTTAGTTGCATATTTAAAACATGTTGAGCTAC
AGCATTATATTCAGCAATTAAGCTCTAAGCCATCCGCAAAAATGACCTCTTATCAAAAGGAGCAATTAAAGGTACTCTCTAATCCTGACCTGTTGGAGTTTGCTTCCGGT
CTGGTTCGCTTTGAAGCTCGAATTAAAACGCGATATTTGAAGTCTTTCGGGCTTCCTCTTAATCTTTTTGATGCAATCCGCTTTGCTTCTGACTATAATAGTCAGGGTAA
AGACCTGATTTTTGATTTATGGTCATTCTCGTTTTCTGAACTGTTTAAAGCATTTGAGGGGGATTCAATGAATATTTATGACGATTCCGCAGTATTGGACGCTATCCAGT
CTAAACATTTTACTATTACCCCCTCTGGCAAAACTTCTTTTGCAAAAGCCTCTCGCTATTTTGGTTTTTATCGTCGTCTGGTAAACGAGGGTTATGATAGTGTTGCTCTT
ACTATGCCTCGTAATTCCTTTTGGCGTTATGTATCTGCATTAGTTGAATGTGGTATTCCTAAATCTCAACTGATGAATCTTTCTACCTGTAATAATGTTGTTCCGTTAGT
TCGTTTTATTAACGTAGATTTTTCTTCCCAACGTCCTGACTGGTATAATGAGCCAGTTCTTAAAATCGCATAAGGTAATTCACAATGATTAAAGTTGAAATTAAACCATC
TCAAGCCCAATTTACTACTCGTTCTGGTGTTTCTCGTCAGGGCAAGCCTTATTCACTGAATGAGCAGCTTTGTTACGTTGATTTGGGTAATGAATATCCGGTTCTTGTCA
AGATTACTCTTGATGAAGGTCAGCCAGCCTATGCGCCTGGTCTGTACACCGTTCATCTGTCCTCTTTCAAAGTTGGTCAGTTCGGTTCCCTTATGATTGACCGTCTGCGC
CTCGTTCCGGCTAAGTAACATGGAGCAGGTCGCGGATTTCGACACAATTTATCAGGCGATGATACAAATCTCCGTTGTACTTTGTTTCGCGCTTGGTATAATCGCTGGGG
GTCAAAGATGAGTGTTTTAGTGTATTCTTTTGCCTCTTTCGTTTTAGGTTGGTGCCTTCGTAGTGGCATTACGTATTTTACCCGTTTAATGGAAACTTCCTCATGAAAAA
GTCTTTAGTCCTCAAAGCCTCTGTAGCCGTTGCTACCCTCGTTCCGATGCTGTCTTTCGCTGCTGAGGGTGACGATCCCGCAAAAGCGGCCTTTAACTCCCTGCAAGCCT
CAGCGACCGAATATATCGGTTATGCGTGGGCGATGGTTGTTGTCATTGTCGGCGCAACTATCGGTATCAAGCTGTTTAAGAAATTCACCTCGAAAGCAAGCTGATAAACC
GATACAATTAAAGGCTCCTTTTGGAGCCTTTTTTTTGGAGATTTTCAACGTGAAAAAATTATTATTCGCAATTCCTTTAGTTGTTCCTTTCTATTCTCACTCCGCTGAAA
CTGTTGAAAGTTGTTTAGCAAAATCCCATACAGAAAATTCATTTACTAACGTCTGGAAAGACGACAAAACTTTAGATCGTTACGCTAACTATGAGGGCTGTCTGTGGAAT
GCTACAGGCGTTGTAGTTTGTACTGGTGACGAAACTCAGTGTTACGGTACATGGGTTCCTATTGGGCTTGCTATCCCTGAAAATGAGGGTGGTGGCTCTGAGGGTGGCGG
TTCTGAGGGTGGCGGTTCTGAGGGTGGCGGTACTAAACCTCCTGAGTACGGTGATACACCTATTCCGGGCTATACTTATATCAACCCTCTCGACGGCACTTATCCGCCTG
GTACTGAGCAAAACCCCGCTAATCCTAATCCTTCTCTTGAGGAGTCTCAGCCTCTTAATACTTTCATGTTTCAGAATAATAGGTTCCGAAATAGGCAGGGGGCATTAACT
GTTTATACGGGCACTGTTACTCAAGGCACTGACCCCGTTAAAACTTATTACCAGTACACTCCTGTATCATCAAAAGCCATGTATGACGCTTACTGGAACGGTAAATTCAG
AGACTGCGCTTTCCATTCTGGCTTTAATGAGGATTTATTTGTTTGTGAATATCAAGGCCAATCGTCTGACCTGCCTCAACCTCCTGTCAATGCTGGCGGCGGCTCTGGTG
GTGGTTCTGGTGGCGGCTCTGAGGGTGGTGGCTCTGAGGGTGGCGGTTCTGAGGGTGGCGGCTCTGAGGGAGGCGGTTCCGGTGGTGGCTCTGGTTCCGGTGATTTTGAT
TATGAAAAGATGGCAAACGCTAATAAGGGGGCTATGACCGAAAATGCCGATGAAAACGCGCTACAGTCTGACGCTAAAGGCAAACTTGATTCTGTCGCTACTGATTACGG
TGCTGCTATCGATGGTTTCATTGGTGACGTTTCCGGCCTTGCTAATGGTAATGGTGCTACTGGTGATTTTGCTGGCTCTAATTCCCAAATGGCTCAAGTCGGTGACGGTG
ATAATTCACCTTTAATGAATAATTTCCGTCAATATTTACCTTCCCTCCCTCAATCGGTTGAATGTCGCCCTTTTGTCTTTGGCGCTGGTAAACCATATGAATTTTCTATT
GATTGTGACAAAATAAACTTATTCCGTGGTGTCTTTGCGTTTCTTTTATATGTTGCCACCTTTATGTATGTATTTTCTACGTTTGCTAACATACTGCGTAATAAGGAGTC
TTAATCATGCCAGTTCTTTTGGGTATTCCGTTATTATTGCGTTTCCTCGGTTTCCTTCTGGTAACTTTGTTCGGCTATCTGCTTACTTTTCTTAAAAAGGGCTTCGGTAA
GATAGCTATTGCTATTTCATTGTTTCTTGCTCTTATTATTGGGCTTAACTCAATTCTTGTGGGTTATCTCTCTGATATTAGCGCTCAATTACCCTCTGACTTTGTTCAGG
GTGTTCAGTTAATTCTCCCGTCTAATGCGCTTCCCTGTTTTTATGTTATTCTCTCTGTAAAGGCTGCTATTTTCATTTTTGACGTTAAACAAAAAATCGTTTCTTATTTG
GATTGGGATAAATAATATGGCTGTTTATTTTGTAACTGGCAAATTAGGCTCTGGAAAGACGCTCGTTAGCGTTGGTAAGATTCAGGATAAAATTGTAGCTGGGTGCAAAA
TAGCAACTAATCTTGATTTAAGGCTTCAAAACCTCCCGCAAGTCGGGAGGTTCGCTAAAACGCCTCGCGTTCTTAGAATACCGGATAAGCCTTCTATATCTGATTTGCTT
GCTATTGGGCGCGGTAATGATTCCTACGATGAAAATAAAAACGGCTTGCTTGTTCTCGATGAGTGCGGTACTTGGTTTAATACCCGTTCTTGGAATGATAAGGAAAGACA
GCCGATTATTGATTGGTTTCTACATGCTCGTAAATTAGGATGGGATATTATTTTTCTTGTTCAGGACTTATCTATTGTTGATAAACAGGCGCGTTCTGCATTAGCTGAAC
ATGTTGTTTATTGTCGTCGTCTGGACAGAATTACTTTACCTTTTGTCGGTACTTTATATTCTCTTATTACTGGCTCGAAAATGCCTCTGCCTAAATTACATGTTGGCGTT
GTTAAATATGGCGATTCTCAATTAAGCCCTACTGTTGAGCGTTGGCTTTATACTGGTAAGAATTTGTATAACGCATATGATACTAAACAGGCTTTTTCTAGTAATTATGA
TTCCGGTGTTTATTCTTATTTAACGCCTTATTTATCACACGGTCGGTATTTCAAACCATTAAATTTAGGTCAGAAGATGAAATTAACTAAAATATATTTGAAAAAGTTTT
CTCGCGTTCTTTGTCTTGCGATTGGATTTGCATCAGCATTTACATATAGTTATATAACCCAACCTAAGCCGGAGGTTAAAAAGGTAGTCTCTCAGACCTATGATTTTGAT
AAATTCACTATTGACTCTTCTCAGCGTCTTAATCTAAGCTATCGCTATGTTTTCAAGGATTCTAAGGGAAAATTAATTAATAGCGACGATTTACAGAAGCAAGGTTATTC
ACTCACATATATTGATTTATGTACTGTTTCCATTAAAAAAGGTAATTCAAATGAAATTGTTAAATGTAATTAATTTTGTTTTCTTGATGTTTGTTTCATCATCTTCTTTT
GCTCAGGTAATTGAAATGAATAATTCGCCTCTGCGCGATTTTGTAACTTGGTATTCAAAGCAATCAGGCGAATCCGTTATTGTTTCTCCCGATGTAAAAGGTACTGTTAC
TGTATATTCATCTGACGTTAAACCTGAAAATCTACGCAATTTCTTTATTTCTGTTTTACGTGCAAATAATTTTGATATGGTAGGTTCTAACCCTTCCATTATTCAGAAGT
ATAATCCAAACAATCAGGATTATATTGATGAATTGCCATCATCTGATAATCAGGAATATGATGATAATTCCGCTCCTTCTGGTGGTTTCTTTGTTCCGCAAAATGATAAT
GTTACTCAAACTTTTAAAATTAATAACGTTCGGGCAAAGGATTTAATACGAGTTGTCGAATTGTTTGTAAAGTCTAATACTTCTAAATCCTCAAATGTATTATCTATTGA
CGGCTCTAATCTATTAGTTGTTAGTGCTCCTAAAGATATTTTAGATAACCTTCCTCAATTCCTTTCAACTGTTGATTTGCCAACTGACCAGATATTGATTGAGGGTTTGA
TATTTGAGGTTCAGCAAGGTGATGCTTTAGATTTTTCATTTGCTGCTGGCTCTCAGCGTGGCACTGTTGCAGGCGGTGTTAATACTGACCGCCTCACCTCTGTTTTATCT
TCTGCTGGTGGTTCGTTCGGTATTTTTAATGGCGATGTTTTAGGGCTATCAGTTCGCGCATTAAAGACTAATAGCCATTCAAAAATATTGTCTGTGCCACGTATTCTTAC
GCTTTCAGGTCAGAAGGGTTCTATCTCTGTTGGCCAGAATGTCCCTTTTATTACTGGTCGTGTGACTGGTGAATCTGCCAATGTAAATAATCCATTTCAGACGATTGAGC
GTCAAAATGTAGGTATTTCCATGAGCGTTTTTCCTGTTGCAATGGCTGGCGGTAATATTGTTCTGGATATTACCAGCAAGGCCGATAGTTTGAGTTCTTCTACTCAGGCA
AGTGATGTTATTACTAATCAAAGAAGTATTGCTACAACGGTTAATTTGCGTGATGGACAGACTCTTTTACTCGGTGGCCTCACTGATTATAAAAACACTTCTCAGGATTC
TGGCGTACCGTTCCTGTCTAAAATCCCTTTAATCGGCCTCCTGTTTAGCTCCCGCTCTGATTCTAACGAGGAAAGCACGTTATACGTGCTCGTCAAAGCAACCATAGTAC
GCGCCCTGTAGCGGCGCATTAAGCGCGGCGGGTGTGGTGGTTACGCGCAGCGTGACCGCTACACTTGCCAGCGCCCTAGCGCCCGCTCCTTTCGCTTTC

Supplementary Table 4 | List of CNVK-modified, fluorophore-labelled imager strands, and docking extension sequences

Table 4a | Sequences for CNVK-modified and fluorophore-labelled imager sequences

In this table, X represents a CNVK-modified nucleotide base.

Strand	Sequence
CNVK-modified imager strand AGv3_P1	5′ – ATACATCTA TC TCGA X GCAT – Cy3b
CNVK-modified imager strand E1v3_P1	5′ – ATACATCTA TC ATCGA X TCAT – Cy3b

Table 4b | Sequences for regular fluorophore-labelled imager sequences

Strand	Sequence
Imager strand for target site quality control AGv3_5′-2	5′ – GAAGCAT – Cy3b
Imager strand for target site quality control AGv3_3′-2	5′ – TCGAAGC – Cy3b
Imager strand for labelling reporter and position marker	5′ – CTAGATGTAT – Cy3b
Imager strand for drift correction marker	5′ – GTAGATTCAT – Cy3b

Table 4c | Sequences for docking extension sequences on DNA origami nanostructures

Strand	Sequence
Docking strand for Action-PAINT candidate labelling target, for AGv3_P1	5′– Staple – TT ATGC T TCGA – 3′
Docking strand for Action-PAINT candidate labelling target, for E1v3_P1	5′– Staple – TT ATGA T TCGAT – 3′
Docking strand for positional marker	5′– Staple – TT ATACATCTA – 3′
Docking strand for 20nm grid drift marker	5′– Staple – TT ATGAATCTA – 3′